Use Authorization

In presenting this thesis in partial fulfillment of the requirements for an advanced degree at Idaho State University, I agree that the Library shall make it freely available for inspection. I further state that permission to download and/or print my thesis for scholarly purposes may be granted by the Dean of the Graduate School, Dean of my academic division, or by the University Librarian. It is understood that any copying or publication of this thesis for financial gain shall not be allowed without my written permission.

Signature _____

Date _____

Investigating the Involvement of Eukaryotic Host Factors in the Translocation of the Tetanus Toxin

by
Cassie L. Thibeault

A thesis

submitted in partial fulfillment

of the requirements for the degree of

Master of Science in the Department of Biological Sciences

Idaho State University

Spring 2015

Committee Approval

To the Graduate Faculty:

The members of the committee appointed to examine the thesis of Cassie L. Thibeault find it satisfactory and recommend that it be accepted.

_____

James R. Groome, Ph.D.

Major Advisor

_____

Caryn Evilia, Ph.D.

Committee Member

_____

James C. K. Lai, Ph.D.

Graduate Faculty Representative

Dedication

To Brian Gentry and Val Bowlden for starting it all.

Acknowledgments

I would like to thank my committee Dr. James Groome, Dr. Caryn Evilia and Dr. James Lai. Thank you also, to the Baldwin Laboratory, the Thomas Laboratory, the Bearden Laboratory and the Molecular Research Core Facility for their contribution of resources.

I am indebted to Dr. Marc Benson for his invaluable guidance, support and wealth of knowledge that contributed greatly to the findings presented here.

Table of Contents

List of Figures

List of Tables

Investigating the Involvement of Eukaryotic Host Factors in the Translocation of Tetanus Toxin

Thesis Abstract-Idaho State Univeristy-2015

Clostridium tetani (*C. tetani*) is the causative agent of the disease tetanus. In an anaerobic environment, germination of *C. tetani* will cause the release of the prominent virulence factor, tetanus neurotoxin (TeNT). TeNT and additional clostridial neurotoxins (CNTs) belong to the AB family of bacterial toxins. However, unlike other members of this toxin family (diphtheria, cholera, and anthrax toxins), host proteins that facilitate translocation of the toxin across the endosomal membrane have yet to be identified. As TeNT is similarly organized and the translocation of the toxin across the endosomal membrane parallels the mechanism of the diphtheria toxin, TeNT may also use the same host protein used by diphtheria toxin, COP1, to facilitate translocation. A protocol to clone, express and purify the catalytic null $TeNT_{RY}$ was successfully optimized. $TeNT_{RY}$ was used to initiate the development of a novel cell-based intoxication assay using the human neuronal cell line SK-N-SH. An immunoprecipitation assay using the neuronal cell line SK-N-SH and the purified $TeNT_{RY}$ was not able to confirm that COP1 facilitates the translocation of TeNT. Additional work is needed to further investigate the relationship between COP1 and TeNT.

Hypothesis and Specific Aims

My hypothesis is that the LC domain of TeNT utilizes the host cell protein COP1 to mediate translocation across the synaptic vesicle membrane. The first aim was designed to purify the necessary amount of toxin to utilize in additional experiments. This was accomplished by cloning and expressing the inactive toxin (catalytic null) $TeNT_{RY,}$ which was then purified *via* affinity chromatography. The second aim was to develop a novel protocol by optimizing a cell-based intoxication assay using the human bone marrow derived neuroblastoma SK-N-SH cell line. To test my hypothesis, the last aim was to determine if the host protein COP1 facilitates $TeNT_{RY}$ translocation by performing an immunoprecipitation assay.

Introduction

Description and Ecology

The disease tetanus was first described in the literature in 430 BC by Hippocrates (56,60). However, it was not until the late 1800's that the etiological agent of tetanus, *Clostridium tetani*, was successfully identified. In 1889, Koch's Berlin laboratory found that a systemic toxin secreted by the bacterium was responsible for the generalized symptoms of tetanus (56). *C. tetani* and other members of the *Clostridium* genus belong to the Fermicute phyla. Fermicutes are classified as bacterial species containing a low (<50%) amount of genomic guanine and cytosine (G+C) (14). Clostridial species belong to a special class of the Fermicutes that are capable of forming heat-resistant endospores. It is the formation of these terminal endospores that give sporulating cells their characteristic drumstick appearance when stained (**Figure 1**).

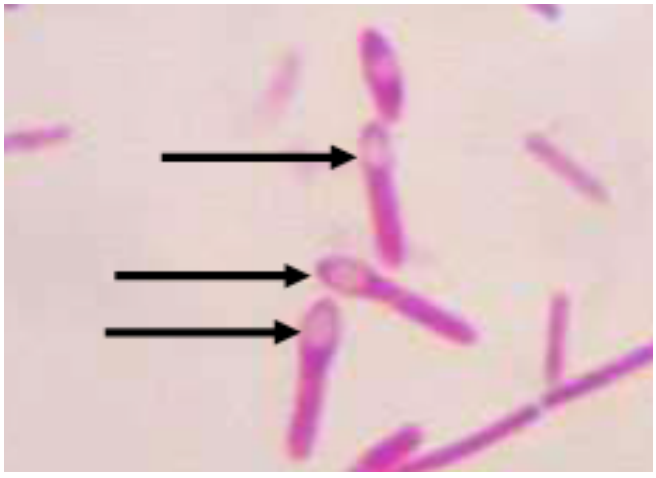

Figure 1. *Clostridium* sp. Gram-stain. The swollen, round sub-terminal endospores (indicated by the arrows) impart a drumstick appearance to the bacteria. Adapted from (44).

Fermicutes are ubiquitous in soil, water and the gastrointestinal tracts of animals (44). As obligate anaerobes, fermentation of amino acids produces alcohols or solvents

as metabolic by-products making some members of the genus industrially significant (14,56). The majority of clostridial species are environmental saprophytic organisms that contribute to the breakdown and recycling of bioorganic material by secreting extracellular enzymes to feed on dead and decaying matter. Nevertheless, they can cause opportunistic infections when introduced into an anaerobic environment (provided by a deep wound) by secreting the same degradative enzymes used in bioorganic material breakdown.

Pathogenic bacteria that belong to the *Clostridium* genus include *C. tetani, C. botulinum, C. difficile* and *C. perfingens* (44). *C. tetani* and *C. botulinum* are the most harmful pathogenic organisms belonging to the genus, as they produce the potent clostridial neurotoxins (CNTs) (44,45). The tetanus toxin (TeNT) and the homologous botulinum neurotoxins (BoNT/A-G) are among the most lethal bacterial toxins known. The estimated 50% lethal dose (LD_{50}) is between 0.1 and 1 ng of toxin/kg of body weight (10,45).

Epidemiology

C. tetani is the etiological agent of localized, generalized, and neonatal tetanus (44,45). Neonatal tetanus has the highest fatality rate (>90%) of any form of tetanus and occurs primarily in underdeveloped countries due to the lack of passive immunity and unhygienic delivery procedures that cause umbilical stump infections (44). Generalized tetanus presents with the classical signs of tetanus including trismus (lockjaw), sardonicus, drooling, and opisthotonos (severe hyperextension and spasticity of the back) (**Figure 2**). This is the most common form of tetanus and is observed in 80% of

cases (45). Without treatment, 15% of patients presenting with generalized tetanus will die (45). Localized tetanus involves sustained muscle contractions only in the affected area and is very rare. This disease also carries the lowest fatality rate (<1%) (46).

Figure 2. Sir Charles Bell's 1809 oil on canvas, *Opisthotonos*. A battle wound infected with tetanus resulting in the severe hyperextension and spasticity of the back. This painting is a depiction of several soldiers suffering from tetanus that Bell treated after the Battle of Corunna. Adapted from (27).

Tetanus is uncommon in developed countries due to the availability of a toxoid-derived vaccine (DTaP) administered during primary immunizations (56,73). According to the World Health Organization (WHO), less than 40 cases of tetanus occurred in the United States in the year 2013 (73). However, the disease remains a major public health issue in underdeveloped nations. In that same year, the WHO reported over 14,000 cases of generalized tetanus and over 4,000 cases of neonatal tetanus occurred

worldwide (73). Of the total tetanus cases reported, close to 80% occurred in underdeveloped nations.

Virulence Factors

Several virulence factors for *C. tetani* are chromosomally encoded. A potent tetanolysin O exotoxin is responsible for the majority of tissue damage associated with tetanus by disrupting the integrity of the host membrane. The exotoxin binds to cholesterol located in the membrane and oligomerizes to form large pores (14). These large pores allow the efflux of ions, metabolites, and proteins that eventually leads to cell death and further promotes tissue destruction. Virulence factors that aid in invasion such as hemolysin and fibronectin-binding proteins are also located on the chromosome (5,14).

C. tetani also contains the large non-conjugative plasmid, pE88, that encodes two important virulence factors. The 114-kDa collagenase enzyme encoded by the *colT* gene is responsible for destroying tissue integrity in the host, allowing the bacterium to avoid the host immune response and gain access to deep tissue (14,29). This provides the necessary anaerobic environment for vegetation of the spore form and production of the second exotoxin, the neurotoxin TeNT. The genes for TeNT (*tetX*) and its direct transcriptional regulator TetR are also located on pE88 (14).

Bacterial Toxins

Toxins, unlike simple chemical poisons, have high molecular antigenicity and distinct modes of action. They are a major virulence factor for bacterial pathogens due to their high specificity for targets that are involved in key cellular functions including

cell signaling, protein translation, cytoskeleton integrity and assembly (38). Their specific modes of action include membrane damage through pore formation, phospholipase activity, inhibition of protein synthesis (N-glycosidase), activation of second messenger pathways (ADP-ribosyltransferase), immune system activation, and proteolytic cleavage (21,34). Bacterial toxins can be classified as either endotoxins or exotoxins.

Endotoxin characterization

Endotoxins are the lipid portion of lipopolysaccharide (LPS) and are released upon lysis of the bacterial cell or are injected directly into the host by means of an injection apparatus (34). LPS is a structural component of the outer membrane of Gram-negative bacteria and is comprised of a sugar core, a species specific sugar chain termed the O antigen, and the heat-stable short fatty acid chain lipid A (21,38). Bacteria containing endotoxins include *E. coli*, *Salmonella* and *Shigella*. Their endotoxins have a general mode of action causing fever, edema, and shock by inducing the host to release cytokines such as interleukin-1 and tumor necrosis factor-α. Endotoxins do not act enzymatically and are therefore less potent then exotoxins, with LD_{50} values on the order of hundreds of micrograms per kg of body weight (21).

Exotoxin characterization

Unlike endotoxins, exotoxins are heat-labile, soluble proteins that are actively secreted into the cellular surroundings by Type I and Type II secretion systems during cell growth, allowing exotoxins to act catalytically on specific targets in areas distant from bacterial growth (38). Their high specificity makes them exceedingly potent and often fatal in even small doses, on the order of one microgram per kg of body weight

(21). Based on their mechanism of action, there are three main categories of exotoxins as described below.

Type I Exotoxins

Type I toxins are superantigens that bind to the host cell surface but are not translocated into the host cell. Superantigens sequentially bind to both the class II major histocompatibility complex (MHC) antigen presenting cells and CD4+ T cell receptors, thus activating T cells to release massive amounts of cytokines resulting in acute conditions of toxic shock, food poising, and fever (52). The toxic shock syndrome toxin (TSST) and the staphylococcal enterotoxins (SE) produced by *Staphylococcus aureus* are well known examples of Type I exotoxins (23,52).

Type II Exotoxins

Type II toxins are phospholipases and pore-forming toxins that disrupt the host plasma and intracellular organelle membranes. Phospholipases, such as the *C. perfringens* alpha-toxin, decrease membrane integrity by cleaving polar head groups of phospholipids in cell membranes (58). Pore-forming toxins including hemolysin and streptolysin O bind to specific membrane receptors, oligomerize and form aqueous pores in the membrane. Aqueous pores cause cells to lyse or release nutrients, aid in delivery of additional bacterial, external factors, or phagosomal escape (26,41).

Type III Exotoxins

Type III, or AB toxins, bind to specific receptors on the host cell surface and are translocated across the host cell membrane to reach an intracellular target. Translocation of the toxin occurs via a channel, or through receptor-mediated

endocytosis. All AB toxins contain at least one A domain and a B domain. The domains are linked by covalent bonds and the toxin is inactive until the covalent bonds are proteolytically cleaved, usually by a host factor (7,22). The enzymatic A domain modifies an intracellular target, causing cell death or altering host cell physiology. The B domain may consist of more than one subunit and binds the toxin to the cell-surface receptors and also plays a role in translocation of the A domain (7,22).

The main bacterial genera responsible for AB toxin mediated diseases are *Clostridium*, *Vibrio*, *Bacillus*, *Escherichia*, and *Corynebacterium* (34). Although the exact intoxication mechanism of clostridial neurotoxins (CNTs) is unknown, those for other AB toxins have been characterized and may serve as models to elucidate the molecular interaction of CNTs within the host cell (**Figure 3**).

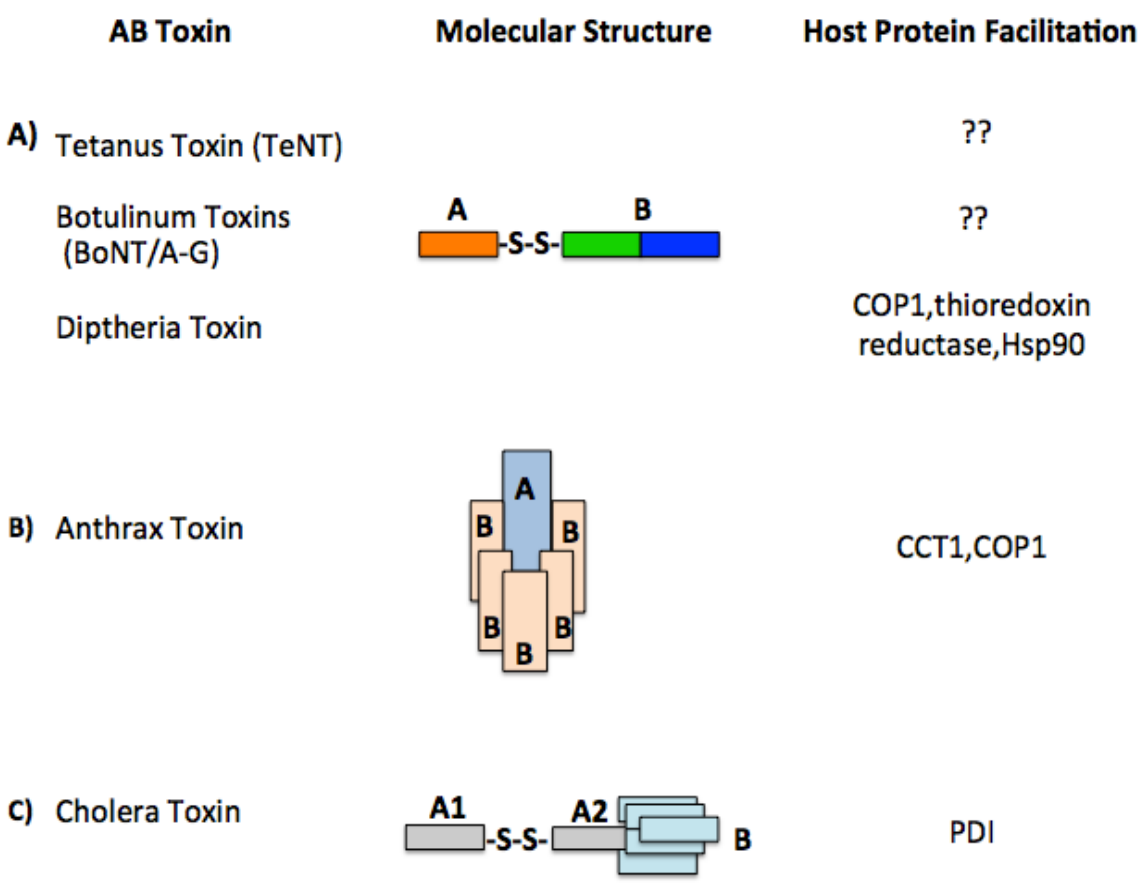

Figure 3. **Comparison of AB toxin models. A**) TeNT, BoNT/A-E and diphtheria toxins are synthesized as a single polypeptide chain comprised of two subunits, an A subunit and a B subunit. COP1, thioredoxin reductase and Hsp90 facilitates entry of the diphtheria toxin across the endosomal membrane while the host protein(s) involved in translocation of TeNT and BoNT/A-E is unknown. **B)** The anthrax toxin is comprised of one A subunit and several B subunits. The toxin utilizes the host protein CCT1 and COP1 to cross the endosomal membrane. **C)** The cholera toxin consists of two A subunits and five B subunits. PDI facilitates toxin entry into the cytosol. Modified from (22).

The cholera toxin (CT) is an AB_5 toxin that contains an A subunit that functions as the catalytic domain and is linked by disulfide bridges to the five B subunits (34,72). The subunits are encoded by separate genes, synthesized separately and are then associated by noncovalent bonds during secretion and binding to the target receptor. CT binds to GM1 gangliosides on the cell surface of the host and undergoes receptor-mediated endocytosis for delivery to the endoplasmic reticulum (ER). The A subunit becomes

separated from the B subunits, unfolds, and is translocated to the host cytosol by proteins involved in the ER associated degradation (ERAD) pathway, specifically protein disulfide isomerase (PDI). Upon entry in the cytosol, the A subunit refolds and targets a G protein-coupled receptor (34,72).

The anthrax toxin is composed of the proteins: lethal factor (LF), edema factor (EF) and protective antigen (PA) that are encoded by separate genes (62,66). The three proteins are synthesized and secreted as separate units that are not toxic until they associate with one another at the target cell surface. PA binds to the receptors ANTXR2 or ANTXR1 on the surface of the host cell. PA is cleaved by the host cell protease furin resulting in heptamerization to form a ring like structure that binds LF/EF (62). The entire PA-LF/EF complex undergoes clathrin-mediated endocytosis. When the lumen of the endosome becomes acidified, PA inserts into the endosomal membrane to form a pore. It is believed that the host chaperonin complex, chaperonin containing t-complex protein 1 (CCT), facilities the translocation of the EF/LF through the PA pore (62,64). Recent evidence has confirmed that interaction of EF/LF with the host's coatomer protein 1 (COP1) complex is also necessary for toxin translocation (66,67).

The diphtheria toxin is synthesized as a single polypeptide chain containing an A domain (catalytic) and B domain (binding and translocation) that are separated by a proteolytic cleavage site (34,43). The toxin recognizes an epidermal growth factor receptor on the surface of the host cell and enters the host cell by clathrin-mediated endocytosis. With acidification of the endosomal lumen, it is hypothesized that the B

domain forms a channel-like structure for the translocation of the A domain that utilizes COP1, thioredoxin reductase and Hsp 90 (34,43,55).

COP1

The COP1 coat structure consists of a heptameric coatomer protein complex that is recruited to the membrane to initiate the collection of cargo proteins (KDEL receptors, p24 family members, SNAREs) and promote vesicle budding (35,40,65). COP1-coated vesicles mediate retrograde transport in the early secretory pathway by trafficking vesicles from the *trans*-Golgi to the ER. They are also responsible for intra-Golgi trafficking (51,65).

As both the TeNT and the diphtheria toxin are organized in a similar fashion, synthesized as single gene peptides, and recent evidence has demonstrated TeNT requires thioredoxin reductase *in vitro*, it is possible that TeNT may also use host COP1 to facilitate translocation (43,45).

Pathogenesis

C. tetani spores are introduced into the host through contamination of deep puncture wounds. Deep puncture wounds provide an anaerobic environment that allows the spores to germinate and release TeNT into the surrounding environment. The toxin enters the blood stream and is delivered to motor neuron axons in the peripheral nervous system. It is trafficked to the central nervous system towards its specific target located in the inhibitory interneuron of the spinal cord (13,36). TeNT is the prominent virulence factor for *C. tetani* (14,34).

TeNT, a Type III exotoxin, is a 150-kDa protein encoded by the *tetx* gene. It is synthesized as single polypeptide chain containing an A domain and B domain (10). The N-terminus of the polypeptide chain is comprised of a ~50-kDa catalytic A domain (a zinc metalloprotease) that is termed the light chain (LC) (8,12). The C-terminus is a ~100-kDa B domain containing two subdomains, the heavy chain translocation domain (HCT) and the receptor-binding domain (HCR) (8).

Although it has been established that synaptic vesicle cycling, specifically clathrin-meditated endocytosis, facilitates TeNT entry into the motor neuron (36) the mechanism of how TeNT exits the motor neuron and enters the inhibitory neuron is unknown.

Synaptic Vesicle Cycling

Efficient synaptic transmission requires rapid delivery of neurotransmitter containing vesicles between presynaptic and postsynaptic neurons (17). Neurotransmitters are housed in presynaptic vesicles, with the exocytosis at the terminal promoted by the arrival of the axonal action potential. High rates of synaptic transmission might exhaust the supply of synaptic vesicles, were it not for their rapid retrieval, and repackaging of transmitters *via* synaptic vesicle cycling (1,3). Thus, both exocytosis and endocytosis are essential components of efficient synaptic transmission.

Successful synaptic vesicle cycling depends on specific soluble *N*-ethylmaleimide-sensitive factor attachment protein receptors (SNAREs) to assemble into a stable, parallel four-stranded superhelical bundle, the SNARE complex, which pulls the vesicle and presynaptic membranes together (38,60). The vesicle-associated membrane protein

(VAMP) synaptobrevin and the presynaptic plasma membrane proteins syntaxin and synaptosomal-associated protein 25-kDa (SNAP-2) are required for exocytosis (**Figure 4**).

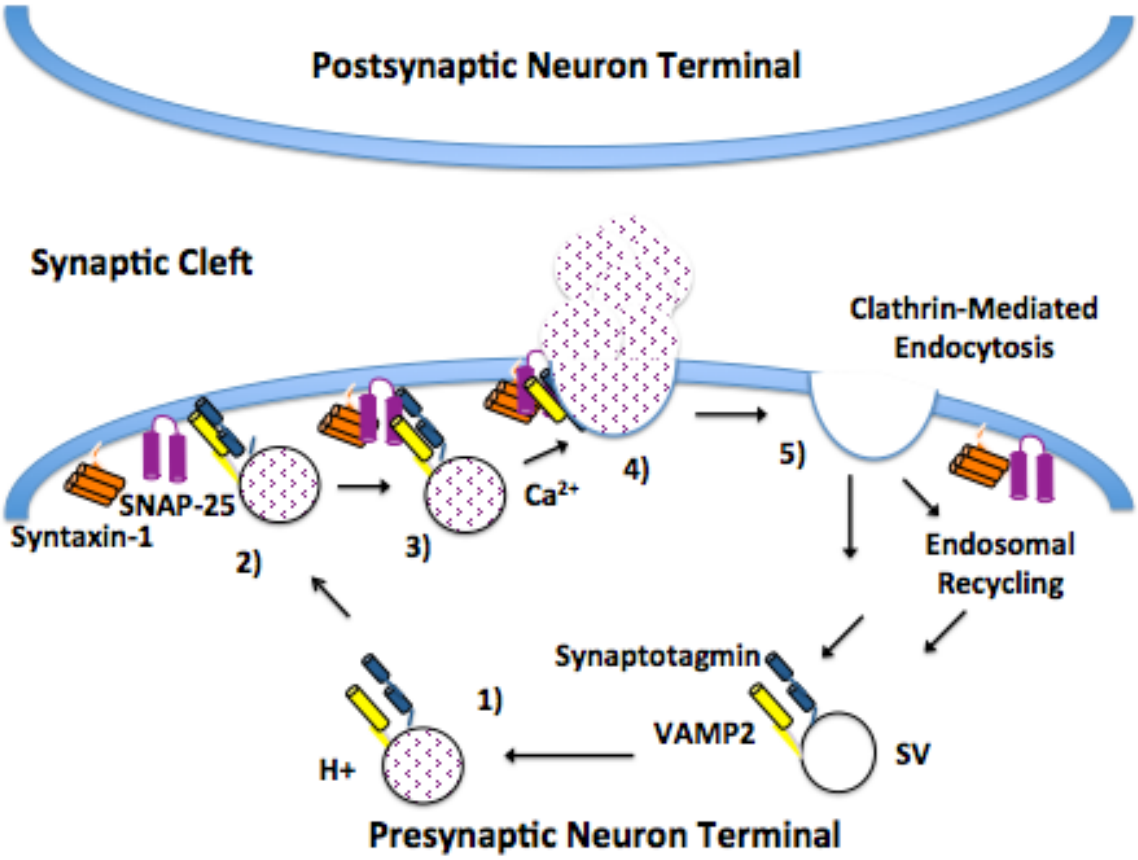

Figure 4. **Synaptic vesicle (SV) cycling.** **(1)** The SV is loaded with neurotransmitters and **(2)** docks to the presynaptic plasma membrane **(3)** where priming occurs via syntaxin-1 assembly with VAMP2 and SNAP-25. **(4)** An influx of Ca^{2+} triggers the binding of synaptotagmin to the SNARE complex and plasma membrane, resulting in rapid fusion and exocytosis of the neurotransmitters. **(5**) After exocytosis, the SV will undergo clathrin-mediated endocytosis. Modified from (63).

Exocytosis

Prior to exocytosis, neurotransmitters are loaded into synaptic vesicles by active transport promoted by an electrochemical gradient established by a proton pump that acidifies the interior of the vesicle (39). The loaded vesicles are docked with the presynaptic plasma membrane and primed for fusion by the partial assembly of the SNARE complex and the presynaptic transmembrane protein syntaxin-1 (57). An action

potential triggers voltage-gated calcium channels to open, causing a highly localized influx of calcium. The rise in intracellular calcium is sensed by the vesicle integral membrane protein synaptotagmin that causes the vesicle to rapidly fuse to the presynaptic membrane by binding the SNARE complex to SNAP-25 (1,3). Once fused, cytoplasmic proteins create a pore connecting the lumen of the vesicle to the synaptic cleft. The neurotransmitter is released and diffuses across the synaptic cleft to bind to specific receptors on the postsynaptic membrane.

Endocytosis

After the contents of the synaptic vesicle have been released, the vesicle is recycled in one of three ways. The vesicles may be reacidified and refilled without undocking ("kiss and stay"), the vesicles may be undocked and recycled locally ("kiss and run") or the vesicles may be endocytosed via clathrin-coated pits (clathrin-mediated endocytosis) (1,57). The latter mechanism is the primary pathway for rapid synaptic vesicle cycling that occurs in nerve terminals (39,63). The vesicular membrane forms a clathrin-coated pit that pinches off with the help of membrane proteins (adaptins) to produce a free clathrin-coated vesicle. The clathrin is removed and the vesicle is reformed and ready to be refilled or passed through an endosomal intermediate where it is broken down and processed into a new synaptic vesicle.

TeNT Intoxication

TeNT enters neuron terminals through what is believed to be direct binding of dual polysialogangliosides receptors in the lipid microdomain of the motor neuron (16,31). Specific arginine and tyrosine residues in the HCR domain of that receptor form

carbohydrate-binding sites for gangliosides GM1a and GD3 (15,16). After binding has occurred, the entire TeNT protein is endocytosed via the clathrin and Rab5-mediated pathway (12,13). The synaptic vesicle containing the internalized TeNT is trafficked in retrograde fashion within the lumen of the neutral endosomes marked with Rab7. An unknown mechanism of transcytosis localizes the synaptic vesicle to the inhibitory neuron (**Figure 5**).

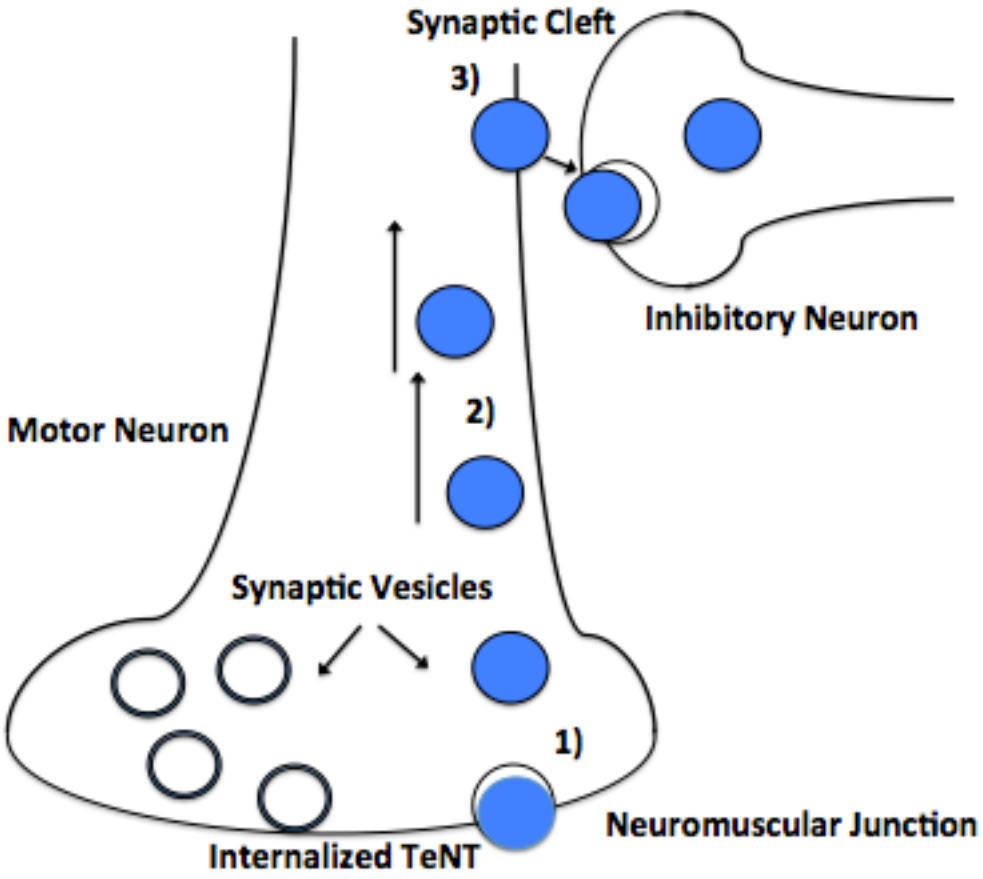

Figure 5. Internalization of TeNT. 1) TeNT follows the dual-receptor binding model and is internalized via SV recycling. **2)** The SV containing TeNT is retrograde trafficked towards the inhibitory neuron. **3)** It is not known how TeNT exits the motor neuron and enters the inhibitory neuron. Modified from (36).

Once inside the inhibitory neuron, the pH drop during synaptic vesicle maturation stimulates formation of the HCT channel to facilitate LC translocation across

the synaptic vesicle membrane. It is unknown if host cell proteins facilitate translocation of LC (11,12,13). LC cleaves VAMP2, thereby inhibiting vesicle fusion to the plasma membrane and subsequent release of inhibitory neurotransmitters such as gamma-aminobutryic acid (GABA, 11,30,). GABA is required for the inhibition of stimulated motor neurons. In the absence of GABA, stimulated motor neurons are unable to be inhibited thus causing unregulated muscle contraction, resulting in the clinical manifestation of tetanus-spastic paralysis (**Figure 6**).

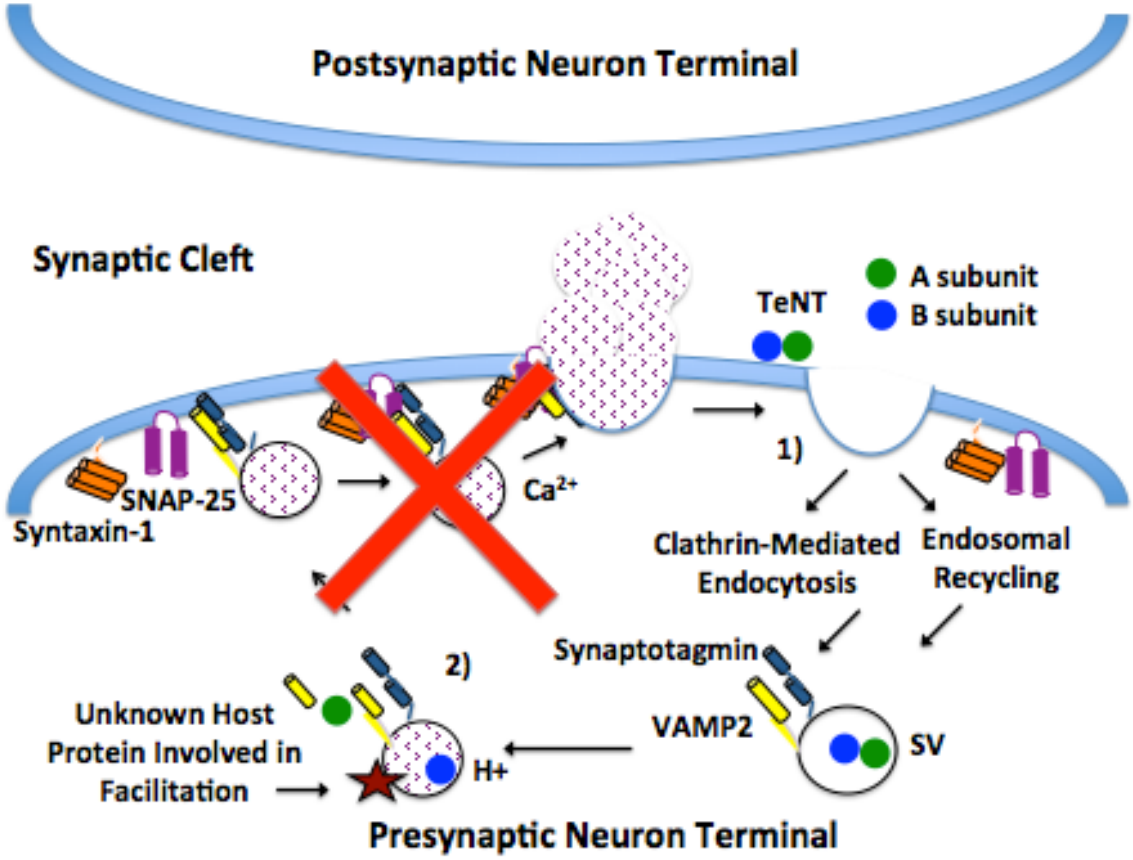

Figure 6. TeNT Mechanism of Intoxication. **1)** TeNT gains entry into the host via clathrin-mediated endocytosis. **2)** Endosome acidification causes the translocation of the A subunit across the endosomal membrane into the host cell cytosol. The A subunit proteolytically cleaves VAMP2, thus preventing the assembly of the SNARE complex. The loaded synaptic vesicle is unable to dock and release neurotransmitters. Modified from (63).

Significance

The known mechanism of action for a toxin can be utilized as model for the mode of action of related toxins. Several AB toxins require host proteins to facilitate the translocation of the catalytic domain across the host endosomal membrane in order to reach their intracellular targets (48). It is likely that TeNT also requires host proteins to facilitate translocation. By confirming the use of host proteins, the exact mechanism of TeNT toxicity could be determined and used as a model for BoNT translocation. BoNT and TeNT share ~35% amino acid identity, exhibit conserved tertiary structure, and the HC of both TeNT and BoNT are nearly identical (**Figure 7**) (12,20,75). In addition, BoNT/B,D,F,G and TeNT not only cleave VAMP2, but BoNT/B and TeNT cleave VAMP2 at the same residue (12,49,50,71). It is unknown how the differential trafficking of the two toxins within the motor neuron occurs.

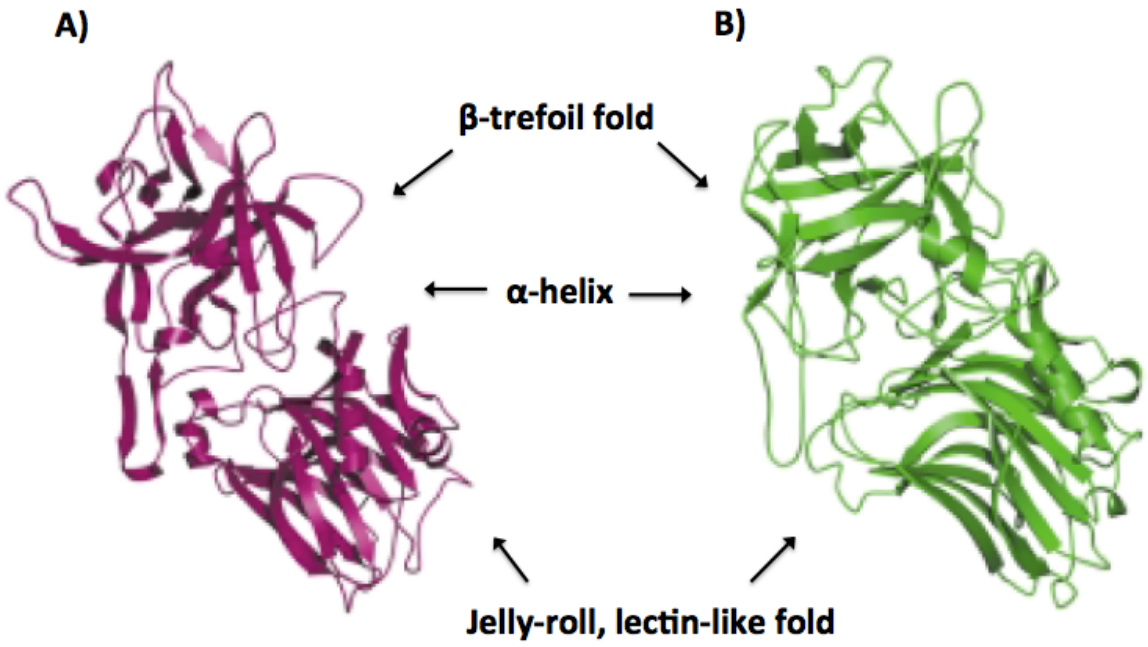

Figure 7. **Crystal structures of TeNT and BoNT/A binding domains.** The N-terminus of the binding domains has jelly-roll, lectin-like folds. The C-terminus of both binding domains has β-trefoil fold and contains the ganglioside-binding sites. Adapted from (71).

Interpretation of BoNT translocation is an important step towards the development of potential vaccines. For example, BoNT is presently classified as a Category A agent and could be used as an effective bioweapon due to the lack of immunity against the toxin (4).

In the last decade, AB toxins have been used as therapeutic agents by exploiting their high specificity in catalytic functions and cell binding as well as their intracellular trafficking properties (2). For example, the B component of AB_5 Shiga toxin, StxB, has the capability to target tumors *in vivo* preferentially over normal tissues due to the overexpression of glycans (specifically Gb3) on the surface of neoplastic cells in colon, pancreatic, ovarian, breast and testicular cancers (7). Specific binding to the cancer cells may allow for StxB to deliver molecular imaging probes and tumor suppressing drugs.

Similarly, recombinant fusion proteins consisting of altered translocation domains of BoNTs are being used to treat chronic pain and chronic obstructive pulmonary disease (11). The BoNT-like binding domain of CNTs could possibly be altered to target non-neuronal cells.

Neurological studies have focused on improvements for the treatment of neurodegenerative diseases such as Parkinson's and Alzheimer's Diseases (2). By utilizing the binding domain of the CNTs, therapeutic nucleic acid sequences may be delivered to the central nervous system to improve on current treatment options that are invasive and have the potential to induce brain damage. Since the binding domain of CNTs are not the catalytically active, it is likely that the synthetic construct would not retain any toxigenic properties but would still be able to bind to the target neuronal cell and undergo endocytosis where it will be delivered to its appropriate CNS target neurons *via* retrograde transport (2).

Materials and Methods

Translation of $TeNT_{RY}$

The plasmid pET28$TeNT_{R372AY375F,}$ containing the synthetic construct of $TeNT_{RY}$ was generously donated from collaborator Dr. Michael Baldwin at The University of Missouri Medical School. The synthetic construct contains a 6x-histdine epitope tag (his tag) on the N-terminus and a streptavidin tag (strep-tag) on the C-terminus. $TeNT_{RY}$ harbors mutations at residues 375 and 378, which were incorporated to prevent the host bacterium, *E. coli*, from mutating $TeNT_{RY}$ back to the pathogenic, wild type form. The mutations produced a catalytic null by replacing crucial amino acids that are involved in transition state stabilization and endopeptidase activity (14,36). The residue at 375 in the wild-type (WT) TeNT contains a polar, hydrophilic arginine (R) while the construct has a nonpolar, hydrophobic alanine (A). The WT TeNT contains the aromatic nonpolar tyrosine (Y) at residue 378 while the construct has aromatic nonpolar phenylalanine (F) (**Figure 8**).

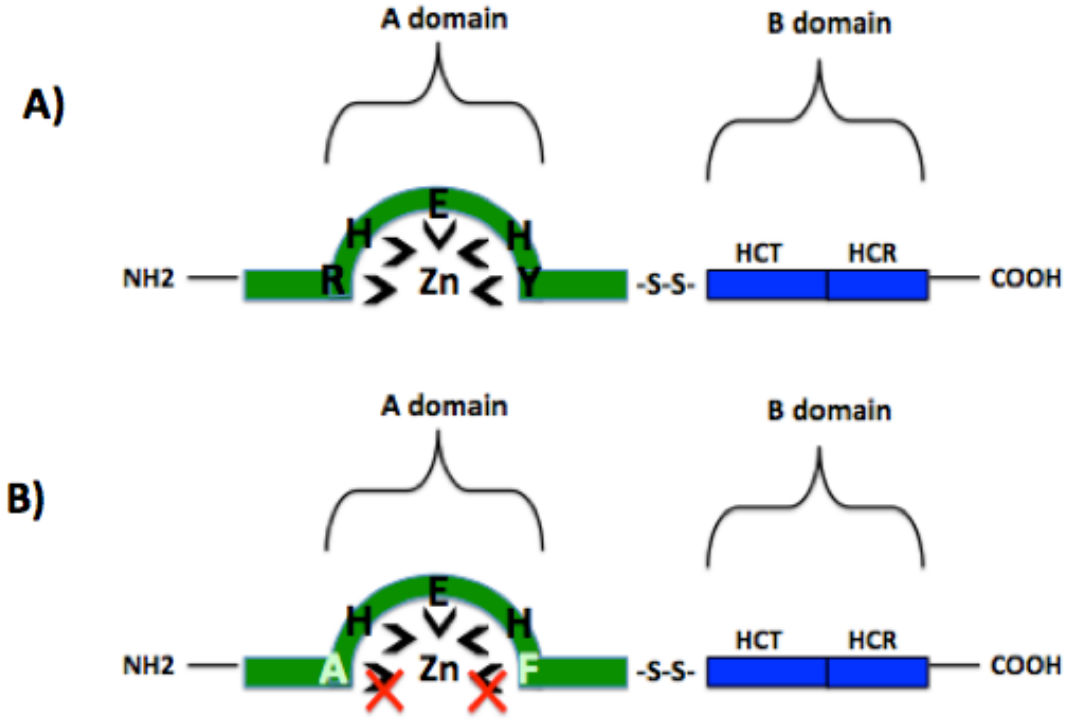

Figure 8. Diagrams of wild-type TeNT and the synthetic construct $TeNT_{RY}$. (A) The wild-type TeNT contains arginine 375 and tyrosine 378 while the construct **(B)** contains alanine and phenylalanine at these loci. Modified from (36).

The reverse sequence of $TeNT_{RY}$ was analyzed using the computer programs Expert Protein Analysis System (ExPASy) and Basic Local Alignment Search Tool (BLAST) to confirm the sites of mutations and calculate the molecular weight of the construct.

Transformation of $TeNT_{RY}$

10 ng of $pET28TeNT_{RY}$ DNA was transformed into the chemically competent cloning cells, DH5α *E. coli*, and the chemically competent expression cells, BL21 *E. coli*, using standard methods. Briefly, the transformation procedure was as such: two separate transformation solutions were produced by combining $pET28TeNT_{RY}$ plasmid DNA in 50 µl of chemically competent DH5α *E. coli* and BL21 *E. coli.* The solutions were incubated on ice for 20 minutes, heat shocked for exactly 30 seconds at 42°C then

returned to ice for additional 2 minutes incubation. The cells were allowed to outgrow for 1 hour at 37°C in Luria Bertani (LB) broth before plating on LB agar containing kanamycin (LB_{Kan}) at 0.05 mg/ml.

pET28 contains an antibiotic resistant gene for kanamycin; therefore, colonies were selected by growth on Luria Bertani (LB) agar containing kanamycin (0.05 mg/ml). Statistically significant colony forming units (CFUs) were observed and isolated colonies were used to inoculate 5 ml of LB kanamycin ($LB_{Kan)}$ broth cultures overnight at 37°C with shaking at 200 RPM. Glycerol stocks were made from the overnight cultures and stored at -80°C for future use.

Table 1. Construct, Strains and Vector Characteristics

Construct	**Genotype/Relevant Characteristics**	**Source/Reference**
$TeNT_{RY}$	Synthetic construct containing mutations at residues 375 and 378	Gift from collaborator Dr. Michael Baldwin
Vector		
pET-28a(+)	pBR322 origin, kan^R, N-terminal His Tag coding sequence, T7 promoter, T7 terminator	Gift from collaborator Dr. Michael Baldwin
Cloning Strain		
DH5α	*E.coli* F- Φ801acZΔM15 Δ(lacZYA-argF) U169 recA1 endA1 hsdR17 (rK-,mK+) phoA supE44λ – thi-1 gyrA96 relA1	Gift from collaborator Dr. Michael Baldwin
Expression Strain		
BL21(DE3)	*E.coli* F- ompT hsdSB (rB-mB-) gal dcm (DE3)	Gift from collaborator Dr. Michael Baldwin

Expression of $TeNT_{RY}$

BL21 pET28$TeNT_{RY}$ was grown overnight in 25 mL of LB_{Kan} at 37 °C with shaking at 200 RPM. The initial 25 ml culture was scaled up to five 200 ml (for a total final volume of 1 liter) LB_{Kan} cultures and incubated at 30°C with shaking at 200 RPM for 2 hours. A

spectrophotometer was used to monitor the optical density at 600 nm (OD_{600}) of the cultures to ensure the bacteria were in the log phase of growth prior to induction. An OD_{600} value between 0.4 and 0.6 is indicative of the optimal cell density. Then, to induce the expression of $TeNT_{RY,}$ 0.5 mM of isopropyl-B-D-1-thiogalactopyranoside (IPTG) was added to the cultures that were then incubated overnight at 16°C with shaking at 200 RPM. The cultures were centrifuged at 10,000 *x g* at 4°C for 10 minutes to sediment the cells. The supernatant was discarded and the cell pellets were stored at -80°C overnight.

A cell lysis solution consisting of Bacterial Protein Extraction Reagent (B-PER; 4 ml per gram of cell pellet, Thermo Scientific, Waltham, MA), DNase I (4 µl per gram of cell pellet, Sigma Aldrich, St. Louis, MO), RNase A (4 µl per gram of cell pellet, Sigma Aldrich) and 1x Halt Protease Inhibitor Cocktail without EDTA (Thermo Scientific) was added to the pellets and allowed to incubate at room temperature for 15 minutes. The suspended cells were centrifuged at 10,000 *x g* at 4°C for 20 minutes. The lysate was passed through a 0.22 µm syringe filter to remove cellular debris.

In a separate protocol, the cells were suspended in a cell lysis solution consisting of nickel affinity binding buffer (20 mM Na_2HPO_4, 300 mM $NaCl_2$, 10 mM imidazole, pH 7.4 at 2-5 ml per gram of cell pellet), DNase I (2-5 µl per gram of cell pellet), RNase A (2-5 µl per gram of cell pellet) and 1x Halt Protease Inhibitor Cocktail without EDTA (2-5 µl per gram of cell pellet). The cell suspension was passed through the French Press three times at 10,000 psi prior to filtering.

Nickel Affinity Chromatography

A 2-2.5 ml column volume (CV) HisPur Ni-NTA Resin (Thermo Scientific) maintained at 4°C was used for purification. The resin was equilibrated with 2 CV of nickel affinity binding buffer before adding the filtered cell lysate. The resin was washed twice with Wash Buffer (25 ml of 20 mM Na_2HPO_4, 300 mM NaCl, 25 mM imidazole), and eluents were collected and stored at 4°C. Finally, up to eight elutions were performed on the remaining bound material using 1 CV of elution buffer (20 mM Na_2HPO_4, 300 mM NaCl, 250 mM imidazole). The collected elutions, wash eluents and flow-through eluents were stored at 4°C and analyzed by SDS-PAGE.

Size Exclusion Chromatography

The concentrated protein sample was further purified by size exclusion chromatography (SEC). The hydrophilic Sephacryl S-200 HR (GE Healthcare, Little Chalfont, United Kingdom) resin was used to pack a glass column (180 ml CV) and allowed to equilibrate overnight at 4°C with elution buffer. The concentrated protein was added at a volume of 1% CV (1.8 ml) and eluted overnight at 4°C. The fractions were collected for every 400 drops, ~10.5 ml; fractions following the void volume (18-36 ml) were analyzed by SDS-PAGE.

Strep-Tactin Chromatography

Following nickel affinity chromatography, the extract was further purified by Strep-Tactin chromatography. A bed volume of 5ml was created using Strep-Tactin Sepharose resin (IBA, Goettingen, Germany) and equilibrated with 2 CV of Buffer W (100 mM Tris/HCL pH 8.0, 150 mM NaCl). Pooled fractions from previous purification steps

were added to the column and the flow-through was collected and stored at 4°C. Five washes were performed using 1 CV of Buffer W. Six elutions were performed using 0.5 CV of Buffer E (100 mM Tris/HCL pH 8.0, 150 mM NaCl 2.5 mM desthiobiotin); fractions were collected and analyzed on SDS-PAGE.

Protein Concentration and Dialysis

Fractions containing a ~150-kDa band corresponding to $TeNT_{RY}$ collected from affinity chromatography were pooled and concentrated using Amicon Ultra-4 Centrifugal Filters Ultracel 10K (Thermo Scientific) and stored at 4°C in 15% glycerol (v/v) for additional purification methods.

Fractions were also dialyzed using Spectra/Por Dialysis Membrane Tubing (Millipore, Billerica, MA). The fractions were dialyzed at 4°C overnight in dialysis buffer (250 mM NaCl, 10 mM HEPES, pH 7.4). An alternate dialysis buffer (20 mM Na_3PO_4, 150 mM NaCl, 40% glycerol) was also used. Dialyzed fractions were analyzed by SDS-PAGE.

BCA Assay

The BCA assay was used to quantitate the total amount of protein present in purified $TeNT_{RY}$ as well as the whole cell lysate fractions of SK-N-SH. Standards for the assay were prepared by diluting stock BSA (2 mg/ml) with 1x PBS for various protein concentrations. Extract samples were prepared by performing 2-fold dilutions with 1x PBS. A standard curve was generated from the absorbance values obtained by the Genesys8 ThermoSpectronic spectrophotometer. The total protein concentration in each sample was calculated from the standard curve using linear regression.

Densitometry

The purified $TeNT_{RY}$ obtained was quantified using densitometry. Various concentrations of the purified protein and the standard Bovine serum albumin (BSA) (Thermo Fisher Scientific, Rockford, IL) were resolved by SDS-PAGE. The Bio-Rad VersaDoc 3000 Imager (Bio-Rad, Philadelphia, PA) was used to determine band intensities. The concentration of $TeNT_{RY}$ was calculated from a standard curve that was produced from the measured band intensities.

SDS-PAGE

SDS-PAGE gels consisted of 10 x 8 cm discontinuous polyacrylamide. The gels were subjected to 75 V (stacking gel) and 90 V (separating gel) using the Hoefer SE250 electrophoresis apparatus containing running buffer (25 mM Tris, 192 mM glycine, 0.1% SDS). The gels were then fixed for 20 minutes at room temperature in a fixing solution (50% methanol, 10% acetic acid). Coomassie Blue solution (50% methanol, 10% acetic acid, 0.1 % brilliant blue G-250) was used to stain the gels for 20 minutes at room temperature. The gels were subjected to a de-staining solution (30% methanol, 10% acetic acid) overnight at room temperature. The gels were visualized using a light box and size estimates were made using the PageRuler pre-stained 2.3 to 250-kDa protein ladder (Thermo Scientific).

Western Blot

Specific primary and secondary antibodies were used to confirm the presence of the N-terminal his tag on $TeNT_{RY}$. Decreasing concentrations of the purified protein were resolved by SDS-PAGE. The gels were rinsed in 1x transfer buffer (25 mM Tris, 192

mM glycine, 20% methanol) and transferred to a nitrocellulose membrane for 1 hour at 4°C using a transfer apparatus set to >300 mA. The membranes were rinsed and probed with the primary antibody, mouse α-histidine (1:2,500, Life Sciences Technologies, St. Petersburg, FL), in a blocking solution of 5% milk in Tris-buffered saline (TBS) overnight at 4°C. The membranes were washed with TBS and probed with the secondary antibody, donkey α-mouse-HRP (1:10,00, Life Science Technologies) in blocking solution for 1 hour at room temperature. The membranes were washed with TBS and incubated for 5 minutes at room temperature with SuperSignal West Pico Chemiluminescent Substrate (Thermo Scientific). The membrane was visualized using the Bio-Rad VersDoc 3000 Imager.

The SK-N-SH expression of COP1 was determined by probing various concentrations of SK-N-SH whole cell lysate with the primary mouse monoclonal anti-COP1 (1:1000, Santa Cruz, Dallas, TX) and secondary goat anti-mouse IgG-HRP (1:10,000, Santa Cruz). To ensure the cells had been adequately lysed, 20 μg of whole cell lysate from mouse brain microvascular endothelial cells from ATCC (Manassad, VA) was also probed. The positive control for COP1 was 50 μg of T24 whole cell lysate (Santa Cruz). All cell lysates were also probed with the primary antibody β-actin-HRP (1:500, Life Science Technologies) that served as a normalizing protein standard.

SK-N-SH Cell Culture

SK-N-SH is a neuronal cell line derived from the metastatic site of a four-year-old female patient with neuroblastoma (9). The cell line was maintained in Dulbecco's Modified Eagle Media (DMEM) supplemented with 10% fetal bovine serum (FBS) and a

penicillin/streptomycin mixture (1:100). The cell line was incubated at 37°C humidified atmosphere with 5% carbon dioxide in 75 ml tissue flasks. The cells were grown until an ~80% confluent monolayer had been reached. Cells were then split using 1x phosphate-buffered saline (PBS) and trypsin (0.25% v/v). The cell suspension was then centrifuged at 200 *x g* for 5 minutes to sediment the cells. The supernatant was removed and discarded; cell pellets were stored at -20°C for future use. Stock cultures in DMEM with 5% DMSO were kept in liquid nitrogen storage.

SK-N-SH whole cell lysate was prepared by suspending thawed cell pellets with modified RIPA Buffer (150 mM NaCl, 50 mM Tris-HCl pH 8.0, 1 mM phenylmethylsulfonlyfluroide (PMFS), 1% Triton X-100, 1% SDS, 1x Halt Protease Inhibitor Cocktail without EDTA, 1 ml per 1 mm of pellet). The suspension was transferred to a chilled microcentrifuge tube and agitated for 30 minutes at 4°C and then centrifuged for 20 minutes at 16,000 x g also at 4°C. Pelleted debris was discarded and the supernatant was stored at -20°C in denaturing buffer following protein quantification by the BCA assay.

In an alternate protocol, SK-N-SH whole cell lysate was prepared by suspending thawed cell pellets with a non-detergent based Lysis Buffer (50 mM Tris-HCL pH 7.4, 150 mM NaCl, 5% (v/v) glycerol, phenylmethylsulfonlyfluroide (PMFS), 1x Halt Protease Inhibitor Cocktail without EDTA). The suspension was incubated on ice for 20 minutes and gently rocked for 30 minutes at 4°C. The lysate was centrifuged for 2 minutes at 16,000 *x g* at 4°C to pellet the debris. The remaining supernatant was subjected to protein quantification via the BCA assay as previously described then stored at -20°C.

SK-N-SH Binding Assay

To prepare for future intoxication studies using the SK-N-SH cell line, binding of $TeNT_{RY}$ to ganglioside loaded SK-SN-SH cells was confirmed. Gangliosides were incorporated into the membrane of confluent SK-N-SH cell cultures by performing a 20 minutes sonication of bovine brain GM1a sodium salt (Santa Cruz, 20 µg/ml) in a 0.5% FBS solution (15ml) followed by a 4 hour incubation at 37°C. The ganglioside-enriched cells were incubated on ice for 30 minutes with ice-cold low-K buffer (15 mM HEPES pH 7.4, 145 mM NaCl, 5.6 mM KCl, 2.2. mM $CaCl_2$, 0.5 mM $MgCl_2$) to prevent synaptic vesicle cycling from occurring and retain synaptic vesicles on the cell surface. The cells were then incubated with 40 nM of $TeNT_{RY}$, fixed in 4% paraformaldehyde in 1x PBS, and permeabilized with 0.1% Triton X-100 in 4% formaldehyde in 1x PBS. The reaction was quenched using 150 mM glycine. Prior to the addition of antibodies, the cells were incubated in a blocking solution (1% BSA (v/v), 0.1% Tween 20 in 1x PBS). Various dilutions (1:50, 1:500, 1:1000) of the primary mouse α-histidine antibody (Thermo Scientific), were incubated overnight at 4°C followed by a 1 hour room temperature incubation of various dilutions (1:50, 1:100, 1:150, 1:200) of the secondary antibody, goat α-mouse IgG fluorescein (Thermo Scientific). A final incubation in 4% paraformaldehyde in PBS was performed. Cells were washed between each step using ice-cold PBS. Cells were viewed using a Leica upright fluorescence microscope.

The results of the initial binding assay demonstrated the need to optimize the titration of the secondary antibody as well as to maintain SK-N-SH cellular integrity. To do this, confluent SK-N-SH cells were incubated at room temperature with fixative (4%

formaldehyde in PBS, pH 7.4), rinsed and washed for 5 minutes with ice-cold PBS, and permeabilized on ice for 20 minutes using 0.1% Tween 20 in PBS pH 7.4. Following a rinse and 8 minutes wash using ice-cold PBS, the cells were incubated for 1 hour with various dilutions (1:50, 1:250, 1:500, 1:750, 1:1000, 1:1500, 1:2000) of the secondary antibody at room temperature and in the dark. A final 8 minutes wash was performed and the cells were viewed. To confirm the optimal secondary antibody dilution had been achieved, the above protocol was repeated as previously described with the inclusion of a 5 minutes room temperature incubation of Hoechst 33342 (Thermo Scientific, 1:1000) following the secondary antibody incubation step. A final 8 minutes wash performed and the cells were viewed.

To determine the optimal titration of the primary antibody, the above protocol was repeated and modified to include the intoxication (40 nM $TeNT_{RY}$) of ganglioside-enriched SK-N-SH cells as previously described. The cells were incubated with various dilutions (1:50, 1:100, 1:200, 1:250, 1:500, 1:750 and 1:1000) of the primary antibody overnight at 4°C. Following a 5 minutes room temperature incubation of Hoescht 33342, the cells were kept away from light and incubated at room temperature for 1 hour with various dilutions of the secondary antibody.

An alternate protocol was attempted to optimize cell fixation and permeabilization on coverslips. SK-N-SH cells were cultured according to the standard protocol. As soon as the cells reached 80% confluence, they were washed with warm PBS and fixed for 15 minutes at 4°C using 4% paraformaldehyde and 4% sucrose in PBS, pH 6.9. The reaction was quenched with 0.1 M glycine, the cells were washed with

warm PBS and permeabilized by adding 0.25% Tween in PBS and incubating at room temperature. The cells were washed with warm PBS and then incubated at room temperature in a blocking solution (heat inactivated 10% BSA in PBS). The primary antibody, anti-NCAM (Thermo Scientific) was diluted in 3% BSA in PBS to a final concentration of 200 µl per cell well and incubate for 1 hour at 4°C. Four, 5 minutes washes were performed using 3% BSA in PBS. The secondary antibody, goat anti-rabbit Alexa488 (Thermo Scientific) was diluted in 3% BSA in PBS to a final concentration of 1:1000 (200 µl per cell well) and incubated for 45 minutes at room temperature without light. The cells were washed for 5 minutes using 3% BSA in PBS and incubated with Hoechst 33342 (1:5000). A final wash with PBS was done and the cells were visualized.

Immunoprecipitation Assay

The possibility of the COP1:$TeNT_{RY}$ interaction was investigated by performing a pull-down assay using the polyhistidine tagged $TeNT_{RY}$ as "bait" and SK-N-SH whole cell lysate as "prey". HisPur Ni-NTA Resin (50 µl bed volume) was applied to three disposable columns (bait:prey, bait-free control, and prey-free control). The columns were equilibrated with binding buffer (20 mM Na_2HPO_4, 300 mM NaCl, 10 mM imidazole, pH 7.4, 1 mM DTT), blocked by BSA (0.5 mg) and rinsed with wash buffer (20 mM Na_2HPO_4, 300 mM NaCl, 25 mM imidazole, pH 7.4). The columns were incubated with $TeNT_{RY}$ (added to saturation, 78.2 µg) and then washed twice to remove unbound $TeNT_{RY.}$ The SK-N-SH cell lysate was added to saturation (248.7 µg) and columns were allowed to incubate for 1 hour. The wash step was repeated and elution buffer (20 mM Na_2HPO_4, 300 mM NaCl, 250 mM imidazole, pH 7.4) was added. All steps were

performed at 4°C. SDS-PAGE was used to analyze all fractions collected at each step. The above protocol was also applied to disposable columns consisting of 250 µl bed volumes of the HisPur Ni-NTA resin.

In an alternate protocol, three (bait:prey, bait free control, and prey-free control) 0.2 ml HisPur Ni-NTA Spin Columns (Thermo Scientific) were equilibrated at 4°C with binding buffer (20 mM Na_2HPO_4, 300 mM NaCl, 10 mM imidazole, pH 7.4). The buffer was removed by centrifugation of the spin columns at 700 *x g* for 2 minutes and incubated with $TeNT_{RY}$ (added to saturation) for 1 hour on an orbital shaker. The columns were spun to remove unbound $TeNT_{RY}$ and incubated with SK-N-SH (added to saturation) for 1 hour on an orbital shaker. The columns were centrifuged to remove unbound lysate and washed two times with wash buffer (20 mM Na_2HPO_4, 300 mM NaCl, 25 mM imidazole, pH 7.4). Three elutions were performed by adding 1 CV of elution buffer (20 mM Na_2HPO_4, 300 mM NaCl, 250 mM imidazole, pH 7.4) and centrifugation of the column at 700 *x g* for 2 minutes. SDS-PAGE and silver staining were used to analyze the fractions collected at each step.

Results

Translation of $TeNT_{RY}$

The nucleotide sequence of the synthetic $TeNT_{RY}$ construct (Baldwin Laboratory) was translated by ExPASy. BLASTP then compared the amino acid sequence of the synthetic construct to the amino acid sequence of the Tetanus Toxin synthetic construct (GenBank accession number AA37720.1) to verify that the two mutations were present. The molecular weight of the construct was also calculated by entering the FASTA sequence of $TeNT_{RY}$ into the Protein Weight Molecular Weight program from Bioinformatics Organization. Using this latter method, the light chain (LC) was calculated at 53.65-kDa and the heavy chain (HC) was 98.3-kDa, similar to the molecular weights of 50-kDa for the LC and 100-kDa for the HC (20) of wild type TeNT.

Induction and Purification of $TeNT_{RY}$

The T7 RNA polymerase encoded by the host strain BL21(DE3) *E.coli*, is expressed with IPTG activation of the *lacUV5* promoter (18). The T7 RNA polymerase directs the expression of the target gene ($TeNT_{RY}$) located downstream of the T7 promoter in the expression vector pET28. The vector also contains a sequence of DNA encoding 6 histidine residues such that the recombinant protein will be produced with an N-terminus his tag.

Expression of BL21 pET28$TeNT_{RY}$ (1-2 L) was induced using 0.5 mM of IPTG as previously described. For initial experiments, the cellular pellets produced by high-speed centrifugation were immediately processed to produce a cleared lysate. I then found that subjecting the cellular pellets to a freeze/thaw cycle (storage at -80°C overnight followed by a 37°C thaw) increased the release of proteins from the cells, as evidenced

by a significant increase in the amount of protein obtained. Ice crystals form during the freezing process and contract during the thawing process, causing the swollen bacterial cells to break.

Purification of BL21pET28TeNT$_{RY}$ soluble cell lysate was achieved by a combination of affinity chromatography techniques (**Figure 9, Figure 10**). Samples containing contaminating or interfering substances obtained for each chromatography procedure were subjected to protein concentration and dialysis for purification.

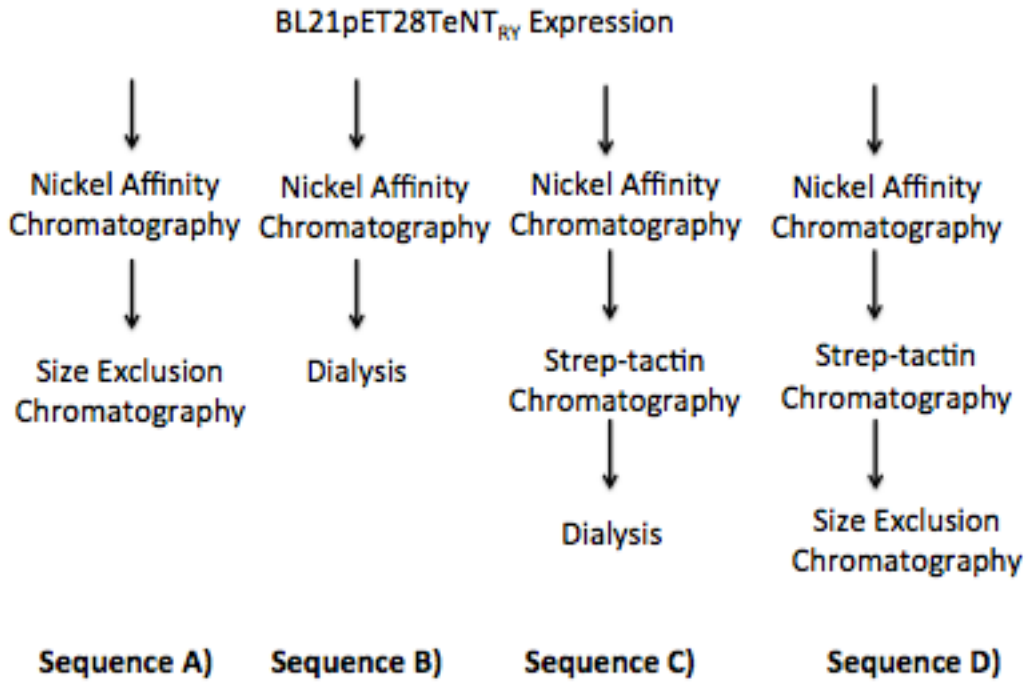

Figure 9. Progression of Purification. Diagram of the four different sequences of purification performed using nickel affinity chromatography, followed by other separation methods.

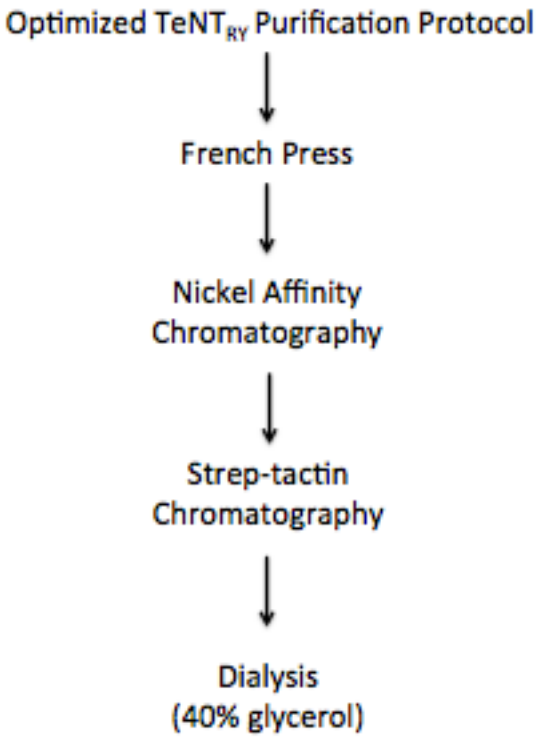

Figure 10. Optimized TeNT$_{RY}$ Purification. Mechanical lysis of the cells by French Press followed by sequential affinity chromatography purification steps utilizing the affinity tags on each terminal of the protein to produce the optimal amount of purified TeNT$_{RY}$. A glycerol based dialysis buffer was employed in the final purification step.

Purification Sequence A

Initial purification of 1 L of BL21pET28TeNT$_{RY}$ was performed by nickel resin affinity chromatography, which utilizes the binding specificity of the his tag on the N-terminus of TeNT$_{RY}$. The HisPur Ni-NTA resin employed in the column contains the chelating resin NTA, which immobilizes the divalent metal nickel ion that will non-covalently bind to histidine. Substances that lack histidine will not bind and be washed through the column. The his-tagged TeNT$_{RY}$ protein is released from the resin by applying an elution buffer containing imidazole, which has a higher affinity for the binding site than histidine.

Using a 2 ml column volume (CV) of equilibrated HisPur Ni-NTA resin, the cleared lysate was eluted in three sequential fractions of 2 ml, 8 ml and 2 ml and visualized on a SDS-PAGE gel (**Figure 11**). The target protein, located by the presence of bands at the 150-kDa weight corresponding to the calculated weight of $TeNT_{RY}$ protein, was present in elutions 1 and 2. These elutions were pooled and concentrated using membrane ultrafiltration to remove impurities present after nickel affinity chromatography. The semipermeable membrane used for ultrafiltration has a specific molecular weight cut off (MWCO) of 10-kDa. Molecules above the specified molecular weight are retained (retent) while smaller molecules are dispersed through the membrane to the filtrate. The resulting concentrated protein (retent) and filtered debris (filtrate) were analyzed by SDS-PAGE (**Figure 11**). The amount of purified protein obtained was too minor to proceed with the needed additional purification.

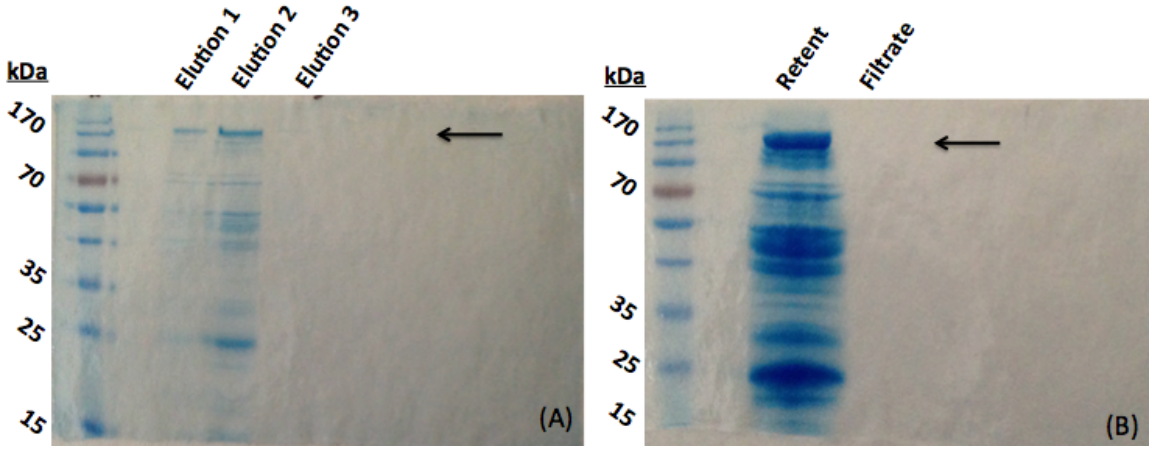

Figure 11. Nickel Affinity Chromatography and Protein Concentration. BL21 pET28$TeNT_{RY}$ soluble lysate obtained from a 1 L culture was applied HisPur Ni-NTA resin (**A**) and eluted in 2 ml, 8 ml, and 2 ml fractions. While the $TeNT_{RY}$ is present (150-kDa bands) there are multiple impurities also present. Fractions containing $TeNT_{RY}$ obtained from Nickel Affinity Chromatography were pooled and concentrated (**B**). While no $TeNT_{RY}$ was collected in the filtrate, an insufficient amount of $TeNT_{RY}$ is in the retent.

Expression of BL21pET28TeNT$_{RY}$ was repeated on a larger scale (1.5 L) in order to obtain a higher concentration of the protein. The soluble lysate was initially purified by nickel affinity chromatography as previously described. The first and second elutions containing the 150-kDa band of TeNT$_{RY}$ were pooled and concentrated resulting in a minor amount of the purified protein (**Appendix A, Panel 1**). Then, the concentrated samples from the former and latter procedure were combined and applied to size exclusion chromatography (SEC) to further resolve the sample.

SEC separates molecules based on size by filtering the sample through a resin containing porous beads. Differential exclusion of smaller molecules such as salts, are retained in the beads due to their ability to travel through the pores while larger molecules cannot penetrate the pores and flow freely through the column.

Approximately 1.8 ml (1% of the SEC 180 ml CV) of the combined protein concentrations were added to the SEC Sephacryl S-200 High Resolution resin and collected in 10.5 ml fractions. Fractions collected after the 40 ml void volume marks were analyzed by SDS-PAGE (**Figure 12**). The 100 to 125 ml volume range containing the 150-kDa bands of TeNT$_{RY}$ were concentrated and analyzed. Purification by SEC decreased the amount of impurities present, but failed to produce an adequate amount of purified TeNT$_{RY}$.

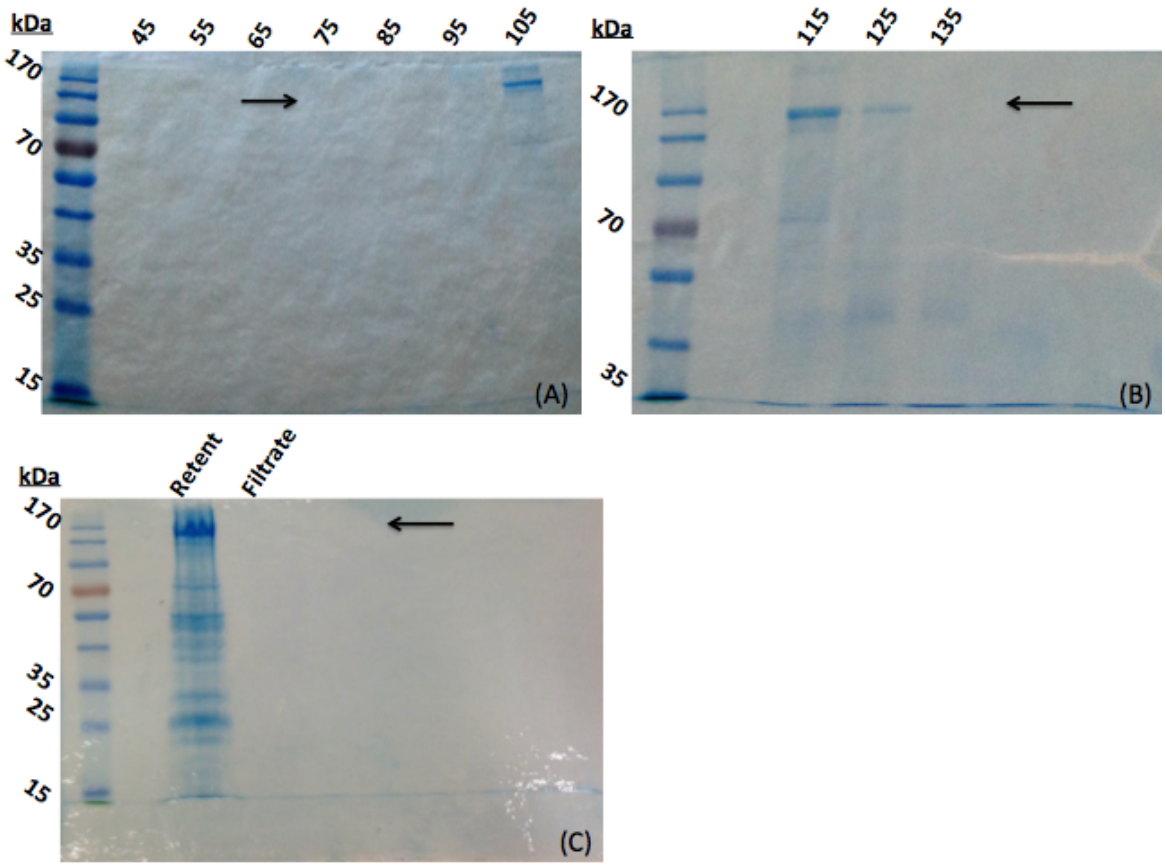

Figure 12. Size Exclusion Chromatography and Protein Concentration. 1.8ml of the concentrated retent was applied to 180 ml of Sephacryl S-200 resin for further resolution by SEC. The fractions collected in the 115 to 135 ml range contained a small amount of $TeNT_{RY}$ (**A,B**), which was combined and concentrated (**C**) resulting in a small amount of $TeNT_{RY}$ recovered and numerous impurities.

The concentrated SEC elutions (600 µl) were subjected to a second round of SEC purification with elutions collected every 2.5 ml to increase the yield of the purified protein. Analysis of the fractions by SDS-PAGE revealed very faint 150-kDa bands present in the 95 to 125 ml range (**Appendix A, Panel 2**). The fractions were combined and concentrated (**Appendix A, Panel 2**). A significant amount of impurities were present in the concentrated fraction; the amount of $TeNT_{RY}$ recovered was slight and too minor to proceed to additional experiments. To clarify the issue existing with the SEC, the column was repacked and calibrated with low-molecular weight proteins.

While the SEC column was being calibrated, a 1 L BL21pET28TeNT$_{RY}$ expression was repeated as previously described and subjected to an alternate protocol of nickel affinity chromatography by incorporating the following changes; four 20 ml washes and 8 elutions of 3 ml each (**Appendix A, Panel 3**). When the elutions were analyzed, very faint 150-kDa bands were observed in elutions 1,2 and 3, indicating the column was not functioning properly or sufficient cell lysis was not occurring. The flow-through and four washes were analyzed by SDS-PAGE to verify the functionality of the HisPur Ni-NTA resin (**Appendix A, Panel 3**). The lack of 150-kDa bands present indicates that the column was working properly. Had the protein been present in the either the washes or the flow-through, it would indicate the protein was not binding to the resin. Although SEC apparently decreased the amount of impurities present, the amount of purified protein decreased. An alternate purification method utilizing dialysis to remove impurities and prevent loss of TeNT$_{RY}$ may work better than SEC. Dialysis removes contaminants by selective and passive diffusion through a semipermeable cellulose membrane. Molecules larger than the diameter of the pore would be retained in the bag while smaller molecules will disperse into the surrounding diaslyate. Thus, I employed dialysis in two subsequent purification strategies.

Purification Sequence B

1.2 L of BL21pET28TeNT$_{RY}$ was expressed and the resulting cellular pellets were frozen at -80°C to increase cell lysis. The cleared lysate was subjected to nickel affinity chromatography as previously described (**Appendix B, Panel 1**). The washes and flow-through were also analyzed to confirm the functionality of the HisPur Ni-NTA resin

(**Appendix B, Panel 1**). To further remove impurities and unwanted smaller molecules, the fractions containing the proteins were pooled and dialyzed overnight in 2 L of Dialysis Buffer (250 mM NaCl, 10 mM HEPES pH 7.4) followed by a 2 hour dialysis in 1 L of fresh Dialysis Buffer. The dialyzed sample was concentrated and analyzed on SDS-PAGE (**Figure 13**). While the dialyzed sample contained a significant decrease in impurities, a minor amount of $TeNT_{RY}$ was obtained. An alternate purification method was needed to further resolve and conserve $TeNT_{RY}$.

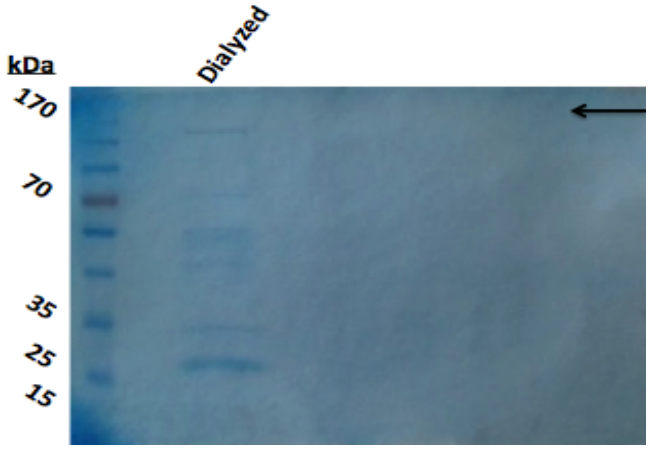

Figure 13. Dialysis. Nickel Affinity elutions containing $TeNT_{RY}$ were combined and dialyzed in 2 L of Dialysis Buffer (250 mM NaCl, 10 mM HEPES pH 7.4). The concentrated, dialyzed sample contained an insignificant amount of $TeNT_{RY}$.

Purification Sequence C

Expression of BL21 pET28$TeNT_{RY}$ was propagated in a 1.6 L culture, the cellular pellets were frozen, and the lysate was initially purified by nickel affinity chromatography consisting of a primary wash of 20 ml, a second wash of 5 ml and one 10 ml elution (**Appendix C, Panel 1**). The elution was applied to a 1 ml CV of Strep-Tactin Sepharose resin (**Figure 14**).

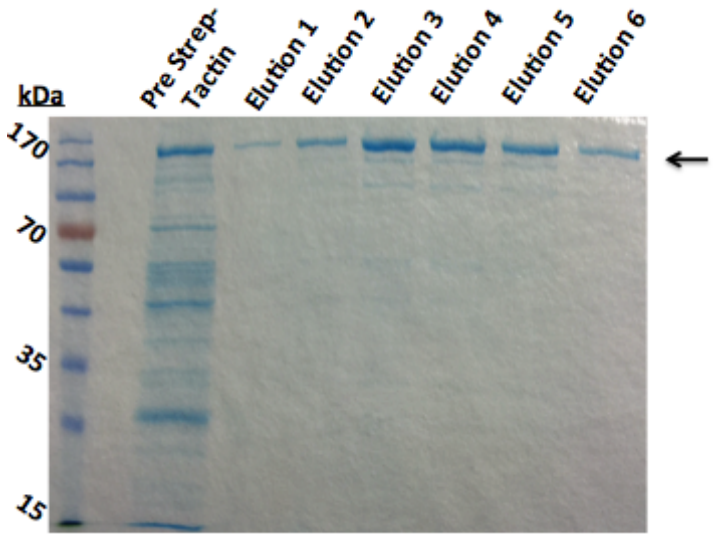

Figure 14. Strep-tactin chromatography. Strep-tactin chromatography was performed on the 10 ml elution obtained from the initial nickel affinity chromatography step. $TeNT_{RY}$ was present in all six 0.5 ml elutions. The amount of impurities present also decreased significantly.

Strep-tactin chromatography was employed as an additional purification step due to the presence of the 8 amino acid (Trp-Ser-His-Pro-Gln-Phe-Glu-Lys) strep-tag on the C-terminus of $TeNT_{RY}$. The affinity strep-tag allows the recombinant protein to be captured by strepavidan (Strep-Tactin resin). The bound protein is competitively eluted by addition of desthiobiotin, a reversibly binding and stable analog of biotin, the natural ligand of streptavidin. Following five 1 ml washes, six 0.5 ml elutions were pooled, concentrated and dialyzed as previously described (**Appendix C, Panel 1)**. SDS-PAGE analysis of the dialyzed sample revealed that sequential affinity chromatography purification steps greatly reduced the amount of impurities while producing an adequate amount of the protein.

The BCA Protein Assay quantified total protein present in the sample. Peptide bonds present in the protein sample reduce Cu^{+2} to Cu^{+1} in an alkaline medium (biuret reaction) producing a purple-colored product when Cu^{+1} chelates two molecules of BCA.

Colorimetric detection of the product occurs at 562 nm and is linear with increasing protein concentrations. Despite the positive outcome of the purification, the minimal amount (40 mM, 0.38 µg) of $TeNT_{RY}$ required for additional experiments was not achieved.

The expression of 1 L of BL21 pET28$TeNT_{\mathbf{RY}}$ and freezing of cellular pellets was repeated as previously described. The lysate was initially purified by nickel affinity chromatography followed by purification by Strep-Tactin chromatography (**Appendix C, Panel 2**). The resulting Strep-tactin elutions were pooled, concentrated and dialyzed. According to the results of the BCA Assay, the final, dialyzed sample contained 53 nM of relatively pure $TeNT_{RY}$. While this was a sufficient amount to proceed to SK-N-SH binding assays, the purification protocol needed to be further optimized to produce a more highly purified and concentrated $TeNT_{RY}$ product.

Purification Sequence D

1.8 liters of BL21 pET28$TeNT_{\mathbf{RY}}$ was expressed in an overnight culture and purified by nickel affinity chromatography as previously described. The elutions containing $TeNT_{RY}$ were pooled and applied to 3 ml of Strep-tactin resin. After the addition of the nickel affinity chromatography elutions, the column was washed five times with 3 ml of wash buffer and six 1.5 ml elutions were concentrated (**Appendix D, Panel 1**) and then applied to 180 ml of SEC Sephacryl S-200 High Resolution resin for SEC as previously described. The fractions containing the 150-kDa protein were combined and concentrated (**Appendix D, panel 2**).

Optimized $TeNT_{RY}$ Purification Protocol

This optimized purification protocol was repeated on a larger scale (expression of BL21 pET28$TeNT_{RY}$ in a 2 L culture) to produce a higher yield of the protein. Thorough lysis of the cell pellets was achieved by storing the initial cell pellets at -80°C overnight then subjecting the lysate to additional mechanical lysis with the French Press. The soluble lysate was purified by both nickel and Strep-Tactin affinity chromatography methods as previously described (**Appendix E, Panel 1**). The final fractions obtained were dialyzed overnight at 4°C in 2 L of a glycerol based dialysis buffer (20 mM Na_3PO_4, 150 mM NaCl, 40% glycerol) and then again for 1 hour at 4°C in 1 L of fresh glycerol based dialysis buffer (20 mM Na_3PO_4, 150 mM NaCl, 40% glycerol). The dialyzed sample was concentrated and analyzed by SDS-PAGE (**Figure 15**). While minor impurities remained at the 130,100, and 55-kDa marks, the final sample appeared to have the most highly purified and concentrated $TeNT_{RY}$ obtained, as was verified by densitometry.

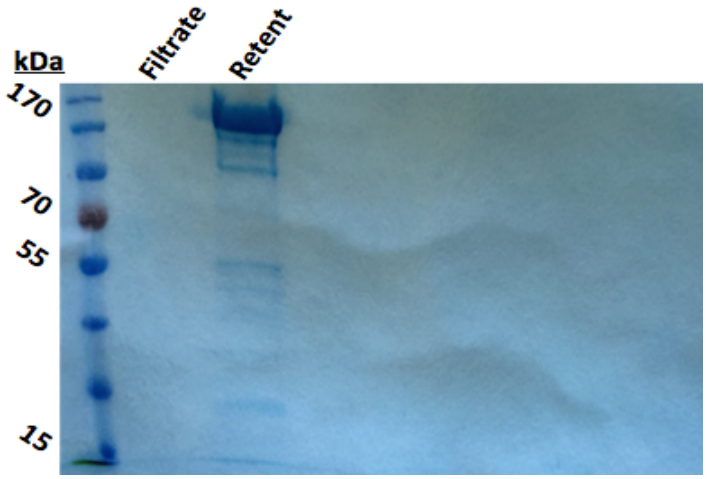

Figure 15. Optimized $TeNT_{RY}$ Purification. Protein Concentration. Sequential affinity chromatography steps were performed on BL21 pET28$TeNT_{RY}$ lysate obtained via French Press. The purified protein was dialyzed in a glycerol-based buffer then concentrated. A significant amount of $TeNT_{RY}$ was recovered. A small amount of impurities were visible at the 130, 100 and 50-kDa marks.

Densitometric analysis was used to quantify the total amount of $TeNT_{RY}$ protein resolved by SDS-PAGE. Image J software measures the intensities of specific bands by comparing band intensities produced from the sample to band intensities from a known concentration of the reference protein BSA. A densitometry value of 411.3 μg/ml confirmed that a sufficient amount of purified protein had been produced by the above protocol (**Appendix E, Panel 2**) to proceed to additional experiments.

Throughout the purification steps, I consistently observed a ~50-kDa band on SDS-PAGE analysis. Since this band may be indicative of proteolytic cleavage of the 50-kDa LC portion of $TeNT_{RY}$ (which corresponds to the placement of the N-terminal his tag), a Western Blot was performed to examine the location of the his tag (**Figure 16**). A 1:2,500 dilution of the primary mouse α-histidine antibody and a 1:10,000 dilution of the secondary donkey α-mouse-HRP were used to probe for the location of the his tag. While the his tag was present at the 150-kDa mark, additional bands representing his tags are also present at the 130, 55 and 50-kDa marks, indicating partial digestion is occurring. However, there remains a significant amount of purified $TeNT_{RY}$ to proceed to additional experiments.

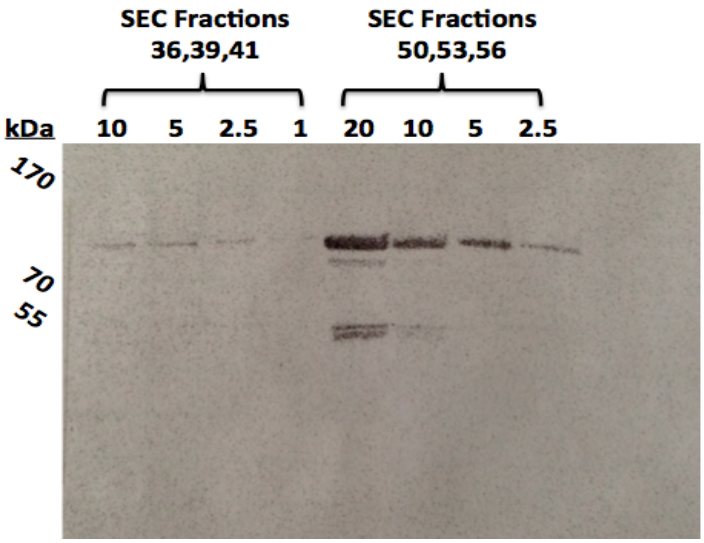

Figure 16. Western Blot Confirmation of His tag on Optimized $TeNT_{RY}$ Purification. The primary antibody, mouse α-histidine (1:2,500) and the secondary antibody, donkey α-mouse-HRP (1:10,00) detected the presence of the N-terminal his tag by the appearance of the band located at 150-kDa.

SK-N-SH Binding Assay Optimization

The exact mechanism of how TeNT enters either of its target neuronal cells (motor and inhibitory neurons) is unknown. However, synaptic vesicle recycling facilitates entry into either neuronal cell. The human neuronal cell line SK-N-SH served as the neuronal model for $TeNT_{RY}$ entry.

The initial intoxication assay that was performed produced inconclusive results. To rule out the occurrence of nonspecific binding by the secondary antibody, a control well consisting of secondary antibody only was tested. To test for SK-N-SH autofluorescence, a control well that contained neither primary nor secondary antibody (SK-N-SH cells only) was included. Since fluorescence was observed in all the wells tested, conditions were optimized for this assay.

The optimal concentration of the secondary antibody was determined by culture, fixation and permeablization of SK-N-SH cells as previously described. Instead of

treating the cultures with GM1a and $TeNT_{RY}$, several dilutions of the goat α-mouse IgG fluorescein secondary antibody (1:50, 1:250, 1:500, 1:750, 1:1000, 1:1500, 1:2000) followed by a short incubation with Hoechst 33342 were performed. Hoechst 33342 is a nucleic acid stain that emits a blue fluorescence when bound to DNA, acting as positive control for the presence of cells. For this control experiment, all the cells were positive for Hoechst stain and negative for all dilutions of the secondary antibody (**Figure 17**), indicating the current protocol was successful.

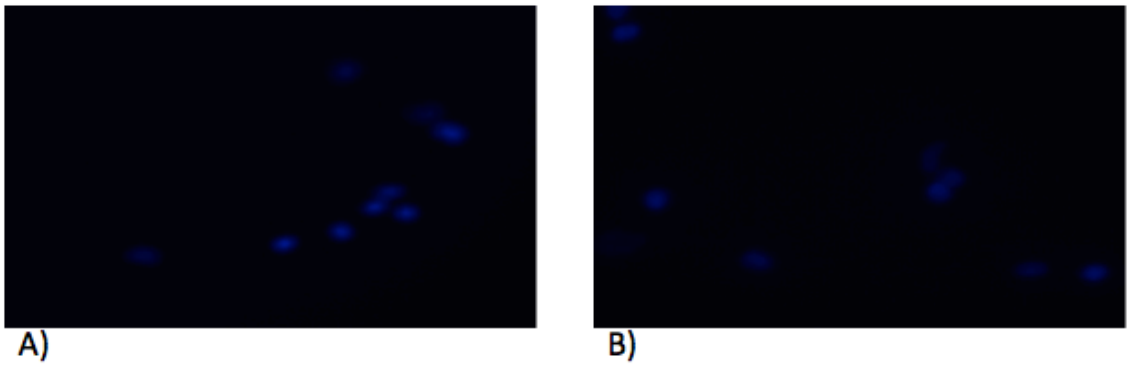

Figure 17. Optimization of the secondary antibody, goat α-mouse IgG fluorescein. (A) The control well consisting of Hoechst stain only was positive, indicating SK-N-SH cells are present. **(B)** The blue color indicates SK-N-SH cells are present while the lack of green indicates nonspecific binding by the secondary antibody is not occurring. Shown is a representative (1:250) of the various dilutions used.

The optimal concentration of the primary antibody was qualitatively determined by culturing SK-N-SH cells followed treatment with GM1a and $TeNT_{RY}$ as previously described. The cells were incubated with dilutions (1:50, 1:100, 1:250, 1:500, 1:750, 1:1000) of the mouse α -his primary antibody overnight followed by an incubation with Hoechst 33342 and an incubation with the goat α-mouse IgG fluorescein secondary antibody (1:1000). The optimal concentration of the primary antibody was found to be 1:100 (**Figure 18**). As the binding assay so far had only been performed in the 6-well

culture plates, a protocol was optimized to allow the experiment to be performed using coverslips as a way to better preserve the cell line.

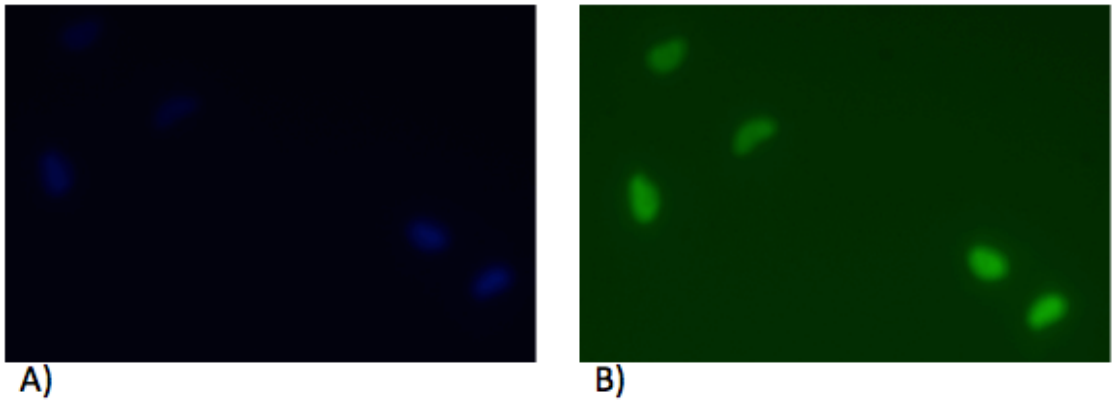

Figure 18. Optimization of the primary antibody, mouse α -his antibody. (A) The control well consisting of Hoechst stain only was positive, indicating SK-N-SH cells are present while the green color **(B)** is indicative of the optimal 1:100 concentration of the primary mouse α -his antibody.

SK-N-SH cells were cultured to 80% confluency in 75 cm^2 plates containing 3 mm glass cover slips. The cells were fixed and permeabilized as previously described. Following blocking, the cells were incubated with the primary antibody, rabbit anti-NCAM, which is an antibody to the cell adhesion molecule involved in neuron-neuron adhesion. The primary antibody was probed with the fluorophore conjugated secondary antibody, goat anti-rabbit NCAM. After the coverslips had been transferred to glass slides, sealed and dried. All the slides were positive for the Hoescht stain and the secondary antibody indicating that the protocol was efficient with the use of coverslips.

SK-N-SH Whole Cell Lysate Optimization

The whole cell lysate prepared using the modified RIPA Buffer produced 1810.3 µg/ml of protein per the BCA Assay. Concentrations from 20 µg to 50 µg of the lysate were then probed for the presence of COP1 while the β-actin-HRP probe was used to

normalize against protein quantity. The positive control for β-actin-HRP, mouse brain microvascular endothelial cells, and the positive control for COP1, T24 whole cell lysate, were also included on the blot. The observed molecular weight of COP1 is 115-kDa, while the observed molecular weight of β-actin-HRP is 32-kDa. When the blot was analyzed, COP1 as well as β-actin was present in all concentrations of the SK-N-SH whole cell lysate indicating the SK-N-SH does express COP1 and the lysate could be used in additional experiments (**Figure 19**).

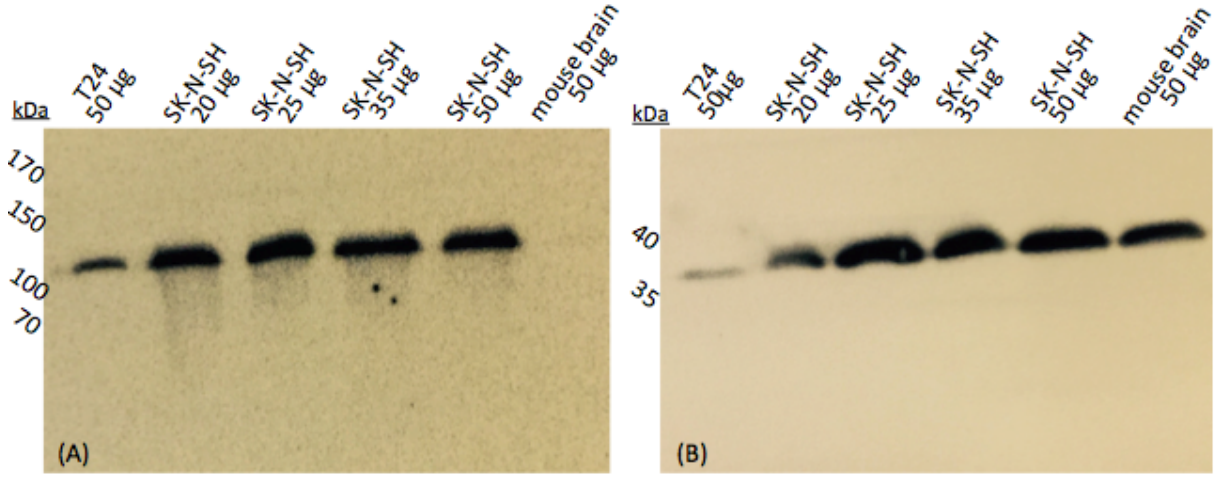

Figure 19. SK-N-SH Whole Cell Lysate Western Blot for COP1. (A) SK-N-SH expression of COP1 is confirmed by the presence of bands at the 115-kDa mark in all three concentrations of whole cell lysate. COP1 is absent in mouse brain microvascular endothelial cells. **(B)** β-actin is represented by bands at the 32-kDa mark.

An alternate protocol required SK-N-SH whole cell lysate to be produced in the absence of detergents in order to be utilized in additional pull-down assays. The whole cell lysate prepared with a non-detergent based Lysis Buffer produced 2.48 mg/ml of protein per the BCA Assay.

Immunoprecipitation Assay

To test for the existence of the $TeNT_{RY}$: COP1 interaction, the purified, tagged $TeNT_{RY}$ functioned as the "bait" and SK-N-SH whole cell lysate containing the potential protein binding partner, COP1, functioned as the "prey" in a pull-down assay. The N-terminal 6x his tag located on $TeNT_{RY}$ was used to bind the bait to immobilized Ni-NTA resin. When SK-N-SH whole cell lysate is added to the bait, the putative binding partner (COP1) for $TeNT_{RY}$ should form a stable complex with the bound $TeNT_{RY}$ that can be eluted and observed on SDS-PAGE. Any unbound protein that has not interacted with $TeNT_{RY}$ will be washed away.

The bait-free control (SK-N-SH whole cell lysate only) was used to ensure that nonspecific binding of SK-N-SH whole cell lysate was not occurring. Then, the prey-free control ($TeNT_{RY}$ only) was used to verify the immobilization of $TeNT_{RY}$ via the Ni-NTA resin. The presence of the 150-kDa $TeNT_{RY}$ observed on SDS-PAGE analysis of the control samples established that the resin effectively binds $TeNT_{RY}$ while the lack of bands present in the whole cell lysate elutions indicates nonspecific binding of the whole cell lysate had not occurred. When the bait:prey elutions were analyzed on SDS-PAGE, $TeNT_{RY}$ was present at the 150-kDa mark (as excepted); three additional bands were also observed (**Figure 20**).

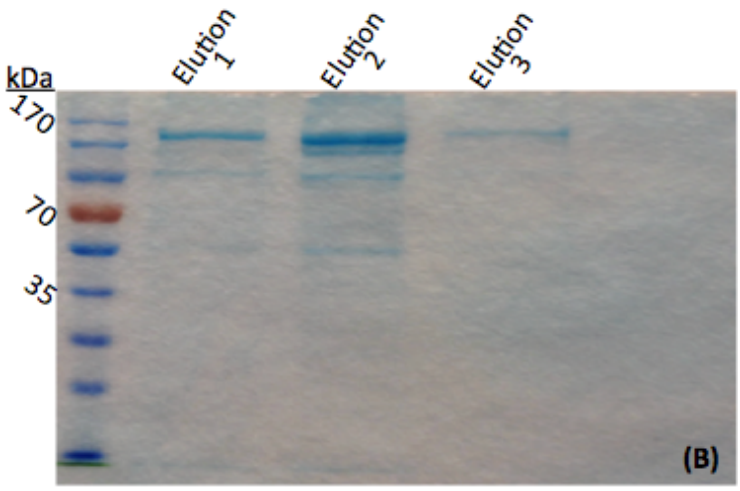

Figure 20. SDS-PAGE analysis of elutions from a Pull-Down Assay. Elutions 1,2 and 3 contain $TeNT_{RY}$ while the 115-kDa COP1 band is absent; elutions 1 and 2 also contain proteins located at the 130-kDa, 100-kDa, and 55-kDa respectively.

Neither of the additional bands appeared to be COP1 as the bands were located at the 130,100, and 55-kDa marks and COP1 is observed at the 115-kDa mark. As COP1 is comprised of subunits, the bands maybe indicative of a specific COP1 subunit that is able to bind to $TeNT_{RY}$ or possibly degraded COP1. COP1 may also be present in such a minor amount, it is unable to be observed using Coomassie staining. However, inspection of the purified $TeNT_{RY}$ obtained (**Figure 15**) showed the presence of bands located at the 130, 100 and 55-kDa marks, indicating a small amount of impurities that were still present in the purified sample may be present in the observed elutions. To further investigate the involvement of SK-N-SH, the pellet that was formed during the initial centrifugation of the SK-N-SH sample with the Lysis Buffer was also subjected to the pull-down assay.

An SDS-PAGE gel was run on the SK-N-SH whole cell lysate and pellet bait:prey elutions and $TeNT_{RY}$, stained with silver to more sensitively detect bands for comparison (**Figure 21**) and analyzed by linear regression. The silver stain shows the 130,100, and

55-kDa proteins are present in $TeNT_{RY}$ alone as well as the bait:prey elutions for both the SK-N-SH whole cell lysate and pellet, indicating they are most likely not putative binding partners of $TeNT_{RY}$. Most likely, these are impurities (partially digested $TeNT_{RY}$) from the $TeNT_{RY}$ sample (**Figure 15, 16**). Linear regression was used to model the relationship between molecular weight and distance migrated for each band under investigation (150, 130,100, 55-kDa). The analysis indicated that the bands present in the bait:prey elutions were nearly identical in molecular weight to the bands present in purified $TeNT_{RY}$, indicating that they are impurities (partially digested $TeNT_{RY}$) from the purified $TeNT_{RY}$.

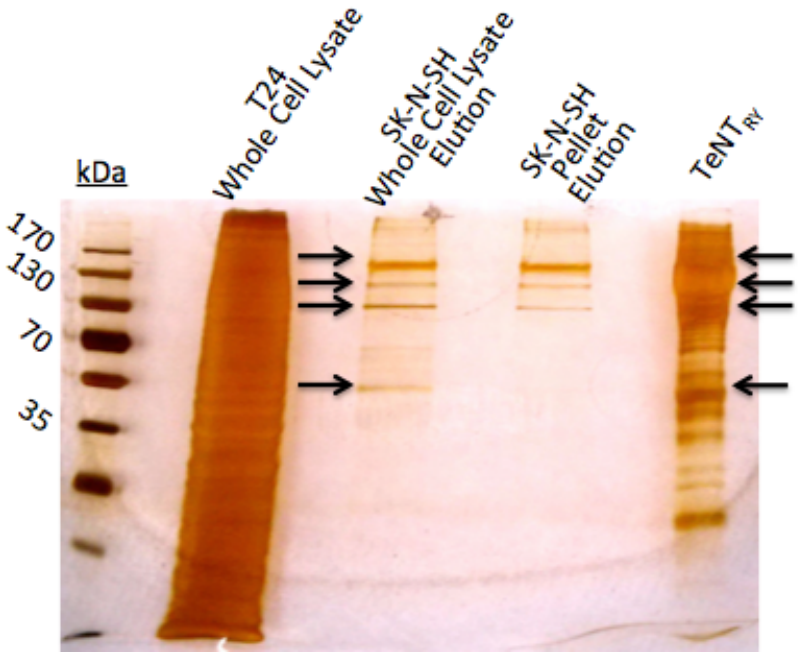

Figure 21. SDS-PAGE Analysis of elutions from a Pull-down Assay, visualized using Silver Stain. The bands that are present in SK-N-SH whole cell lysate and pellet elutions do not appear to contain putative binding partners, as the same bands are also present in $TeNT_{RY}$.

Discussion and Future Directions

The principal virulence factor, the neurotoxin TeNT, of *C. tetani* belongs to the AB family of bacterial toxins, which include the diphtheria, cholera, anthrax and botulinum toxins. The majority of these toxins have known host proteins that facilitate the translocation of the toxin across the hosts' endosomal membranes (43,45). However, the host protein involved in the translocation of TeNT is unknown. A single gene encodes the subunits for the TeNT toxin and diphtheria toxin and both toxins require thioredoxin reductase, the mechanism of intoxication may be similar. Therefore, I hypothesized that TeNT uses the same host protein used by diphtheria, COP1, for translocation. The goal of this research was to determine if COP1, expressed from the neuronal cell line SK-N-SH, could be involved in the translocation of $TeNT_{RY}$ by confirming the existence of COP1:$TeNT_{RY}$ interaction.

The first goal was to develop a novel purification protocol for $TeNT_{RY}$. A novel protocol utilizing sequential affinity chromatography methods was successfully established that resulted in an adequate amount of purified $TeNT_{RY}$ for additional experiments. The purification was further optimized with the addition of a glycerol-based buffer used in the dialysis of the final protein. However, a small amount of degraded $TeNT_{RY}$ was still present in the final product (**Figure 15**). While this did not interfere with additional experiments, their presence in the pull-down assay required a silver stain (**Figure 20**) and linear regression to be performed in order to confirm they were in fact products in the original purified sample. The optimized purification scheme (**Figure 9**) presented here could be repeated with an N-terminal GST tag instead of an N-

terminal His-tag with the exception of GST-tag affinity chromatography instead of nickel affinity chromatography.

The second goal was to develop a novel-cell based intoxication assay using the human neuronal cell line, SK-N-SH, and purified $TeNT_{RY}$. The initial experimental design for the intoxication assay addressed two factors: how well $TeNT_{RY}$ binds to GM1-loaded SK-N-SH membranes and, the cellular entry of $TeNT_{RY}$ by receptor-mediated endocytosis. However, a novel-cell based intoxication assay was successfully optimized for the 4°C treatment only, while only the parameters for the 37°C treatment were optimized. The concentrations of the primary and secondary antibodies were established as well as a protocol for cell fixation to coverslips. Future work should focus on implementing the established parameters in an intoxication assay that is performed at 37°C, the temperature receptor mediated endocytosis occurs, allowing $TeNT_{RY}$ intoxicated vesicles to be isolated for additional immunoprecipitation assays. Current work on TeNT utilizes PC12 cells or rat brain homogenate as the gold standard for neuronal models (12,13); SK-N-SH represents an alternate neuronal model.

In addition, this work established that SK-N-SH has the potential to be used in research involving vesicular transport. Genetic analysis in yeast and biochemical analysis of *in vitro* reconstituted membrane transport reactions have allowed for the discovery of how proteins move between compartments during secretion and vesicle formation. However, much is unknown regarding the regulation and function of synaptic vesicles, the specific mechanism of transport vesicle formation, and recycling (1,3,46). Furthermore, since SK-N-SH expresses COP1, this cell line could be used to investigate

COP1 vesicle function to elucidate factors that are involved in COP1-dependant transport.

The last goal was to determine if the host protein COP1 facilitates the translocation of $TeNT_{RY}$ by performing an immunoprecipitation assay utilizing purified $TeNT_{RY}$ and SK-N-SH. SK-N-SH whole cell lysate (prey) was added to $TeNT_{RY}$ (bait) that was immobilized on Ni-NTA resin. If COP1 was a binding partner, it would have bound to the immobilized $TeNT_{RY}$ creating a complex that would be eluted out and visualized on SDS-PAGE and confirmed by Western Blotting. While my results suggested that COP1 does not interact with $TeNT_{RY}$, these results are inconclusive. There are several limitations for the interpretation of the results discussed below.

Technical Limitations

While an adequate amount of purified $TeNT_{RY}$ was used as bait, verification of the degraded $TeNT_{RY}$ product did have to be confirmed. A purified $TeNT_{RY}$ sample that contained little to no degraded products may provide a better bait option. While the N-terminal histidine affinity tag provides a good option for purification, $TeNT_{RY}$ may be sequestering the divalent nickel cation that is used in the resin. This would interfere with $TeNT_{RY}$'s ability to be translocated across the mechanism and interaction with putative binding partners may not be observed. Second, to provide conclusive evidence, the cellular fractions of intoxicated SK-N-SH should be harvested and collected by differential centrifugation and used in coimmunoprecipitation assay where an anti-COP1 antibody as bait and the various fractions of the intoxicated SK-N-SH cell components as prey will be used to detect COP1-TeNT interactions. The complex could then be

observed on a native PAGE gel or obtained by size exclusion chromatography. The TeNT substrate synaptobrevin would serve as a positive control for fidelity of the coimmunoprecipitation.

COP1 Limitations

COP1 itself (coat complex components, vesicle formation, cargo, vesicle destination) remains poorly understood. While it is known that the COP1 coat complex is comprised of heptameric (α,β,β',γ,δ,ε,ζ) coatomer complexes that form 2 subclasses (6,61). The trimeric complex (α,β',ε) constitutes the outer layer of the COP1 coat while the tetrameric complex (β,γ,δ,ζ) constitutes the inner layer of COP1 (6). Recent evidence has identified the existence of isoforms of γ and ζ (6). An immunoprecipitation assay should include anti-bodies not only to the widely used coatomer complexes but the isoforms as well. In addition, while these isoforms still assemble into functioning COP1 vesicles, they impart a distinct subcellular localization (6). In essence, these different COP1 coats serve different transport routes and traffic to different compartments. Recent research has also confirmed there are two distinct populations of mammalian COP1, ER-destined COP1 and intra-Golgi COP1, that differ in their receptors, cargo, and tethering specificity (6,61). Future proteomic analysis of specific COP1 vesicle populations would reveal information pertaining to coat assembly (particularly isoform involvement), cargo, and destination that are necessary to understand COP1 transport.

TeNT and COP1 may also not interact *in vitro* due to contaminants in the lysate. The antibody recognizes COP1 in the lysate, but the TeNT recognition may be for a different epitope than for the antibody that is suppressed by impurities in the lysate.

Finally, the TeNT and COP1 interaction may exist, but the degradation of TeNT may render such interaction less effective as a consequence of decreased quantity of functional TeNT, or as a consequence of degradation product interference with the interaction itself.

SK-N-SH Limitations

The lack of apparent binding of TeNT to COP1 may be due to the lack of interaction of COP1 and TeNT *in vivo*. If TeNT only interacts with specific isoforms of COP1 as discussed above, these isoforms may not be present in SK-N-SH. As the chemical nature of the putative binding partner of TeNT is unknown, the relative abundance of the biding partner in neuronal cells remains unknown. Therefore, SK-N-SH may not be expressing the binding partner for TeNT at all. The SK-N-SH cell line does interconvert between two morphologically and biochemically distinct cell populations; neuroblastic (N) cells and substrate-adherent (S) cells (9). The N cells are neuronal like, while S cells lacked neuronal characteristics and both cell populations are homogenous with other neuroblastoma cell lines (9). As the cell cultures are grown to confluency, the N cells are expressed in a higher number. Perhaps, the binding partner of TeNT is expressed in a specific cell phenotype and differentiation will be required for expression to occur.

Novel Mechanism

COP1 is required for translocation of the AB toxins diphtheria and anthrax (64,67,68). These toxins also contain a conserved T1 entry motif that is required for the interaction with COP1 for translocation (54,69). Because there are factors that remain unknown in COP1, TeNT may also posses an entry motif to a yet unknown component of COP1 (isoform). In addition to COP1, diphtheria requires Hsp 90 and thioredoxin reductase while anthrax requires GRP78 (BiP) (64,67,68). Because COP1 alone is not sufficient for translocation of the above AB toxins, there may be additional proteins that interact with COP1 that are involved in the translocation of TeNT that have not been identified preventing the observation of COP1 involvement. Specific membrane proteins are required for the successful fusion of vesicles to their respective targets (clathrin coated vesicles require adaptins) (61). It could be that these proteins are required for the interaction of TeNT and COP1, however, membrane proteins required for COP1 remain unknown. Alternatively, TeNT could be using an intoxication mechanism that is novel to the AB family of toxins but is used by other endocytic pathways. In order for TeNT to reach its cytosolic SNARE target, TeNT has to retrograde traffic through the motor neuron to the inhibitory neuron before the LC is translocated across its endosomal membrane (59). It is possible that TeNT translocation per se is dependent on cargo proteins yet to be identified that allow the toxin to undergo long-range axonal transport that ultimately leads to its cytosolic delivery within the inhibitory neuron. It is able to do so For example, many viral families such as Picornaviridae, Rhabdoviridae, Herpesviridae, and Adenoviridae utilize this entry strategy to gain access via an

endosomal entry pathway in the motor neuron that retrograde trafficks the virus to specific neurotrophin receptors located in the CNS (12,59). TeNT could be using a COP1-independent pathway that other members of the AB toxin family use. For example, the shiga toxin utilizes the Rab6-depenent retrograde trafficking route for toxin delivery and translocation (7). The pertussis toxin uses host ERAD pathway, but unlike the cholera toxin, it does not contain a KDEL receptor that targets its delivery to the ERAD pathway (7). It is unknown at this time how the toxin is able to infiltrate this pathway. Perhaps, an unknown COP1-dependent pathway is being used.

Conclusion

The tetanus neurotoxin produced by *C. tetani* contributes significantly to the bacterium's virulence. TeNT is an AB toxin and like the majority of AB toxins, it may rely on host factors to facilitate translocation into the cytosol to reach its target. $TeNT_{RY}$ was cloned, expressed and purified using affinity chromatography. An intoxication assay was performed and optimized at using fluorescently labeled anti-histidine antibodies to confirm $TeNT_{RY}$ binding (4°C). An immunoprecipitation assay was performed on SK-N-SH whole cell lysate and $TeNT_{RY}$ to examine if TeNT interacts with COP1. While the results suggest that COP1 may not be involved in the translocation of TeNT, further testing is required to confirm this hypothesis. One such test could be a genetic knock-out of COP1 in the cell line to test whether or not these cells retain, or lose, their intoxication potency.

The AB neurotoxins produced by *C. tetani* and *C. botulinum* have highly conserved structures suggesting the mechanism of translocation for tetanus and botulinum are similar (13,36,45). This similarity may allow the elucidation of BoNT translocation using the safer alternative, TeNT. Furthermore, if the mechanism of CNT translocation is similar for all members of the AB toxin family, a universal therapeutic may be developed to combat AB toxin-mediated diseases (13,34,42). It may also be used to ascertain a novel cellular pathway for transport across the endosomal membrane.

References

1. **Alabi, A.A., Tsien, R.W.** 2012. Synaptic vesicle pools and dynamics. Cold Spring Harb Perspect Biol. 4**(8):**a013680.

2. **Andreu, A., Fairweather, N., Miller, A.D.** 2008. Clostridium neurotoxin fragments as potential targeting motieties for liposomoal gene delivery to the CNS. ChemBioChem. **9**:219-231.

3. **Balch, W.E., Dunphy, W.G., Braell, W.A., Rothman, J.E.** 1984. Reconstitution of the transport of protein between successive compartments of the Golgi measured by the coupled incorporation of N-acetylglucosamine. Cell **39**: 405-416.

4. **Baldwin, M.R., Tepp, W.H., Przedpelski, A., Pier, C.L., Bradshaw, M., Johnson, E.A., Barbieri, J.T.** 2008. Subunit vaccine against the seven serotypes of Botulism. Infect. Immun. **76**(3): 1314-1318.

5. **Barbieri, J.T.** 2013. Damage by microbial toxins. *In* Engleberg, N.C., DiRita, V.J., Dermody, T.S**.,** Rhyner, S. (ed), Schaechter's Mechanisms of Microbial Disease*,* 5th ed, Wolter Kluwer, Baltimore, MD.

6. **Beck, R., Rawet, M., Wieland, FT., Cassel, D.** 2009. The COP1 system: molecular mechanisms and function. FEBS Lett. **583**:2701-2709.

7. **Beddoe, T., Paton, A.W., Le Nours, J., Rossjohn, J., Paton, J.C.** 2010. Structure, biological functions and applications of the AB_5 toxins. Trends Biochem Sci*.* **35**:411-418.

8. **Benson, M. A., Fu, Z., Kim, JJ, Baldwin, M. R.** 2011. Unique ganglioside recognition strategies for clostridial neurotoxins. JBC. **286**:34015-34022.

9. **Biedler, J.L., Roffler-Tarlov, S., Schachner,M., Freedman, L.S**. 1978. Multiple neurotransmitter synthesis by human neuroblastoma cell lines and clones. Cancer Research. **38**: 3751-3757.

10. **Binz, T., Rummel, A.** 2009. Cell entry strategy of clostridial neurotoxins. JNC. **109**:1584-95.

11. **Binz, T., Sikorra, S., Mahrold, S.** 2010. Clostridial Neurotoxins: Mechanism of SNARE cleavage and outlook on potential substrate specificity reengineering. Toxins. **2**:665-682.

12. **Blum, F.C., Chen, C., Kroken, A.R., Barberi, J.T.** 2012. Tetanus toxin and Botulinum toxin A utilize unique mechanisms to enter neurons of the central nervous system. J IAI. **80**:1662-1669.

13. **Blum, F.C., Ptrzedpelski, A., Tepp, W.H., Johnson, E.A., Barbieri, J.T**. 2013. Entry of a recombinant, full-length, atoxic Tetanus neurotoxin into Neuro-2a cells. Infect. Immun. **82**(2):873.

14. **Bruggeman, H.** 2003. The genome sequence of Clostridium tetani: the causative agent of tetanus. PNAS. 100.3:1316-321.

15. **Chen, C., Baldwin, M., Barberi, J.T.** 2008. Molecular basis for Tetanus toxin coreceptor interaction. Biochemistry. **47**:7179-7186.

16. **Chen, C., Fu, Z., Kim, J.P., Barberi, J.T., Baldwin, M.R.** 2009. Gangliosides as high affinity receptors for Tetanus neurotoxin. JBC. **284**:26569-26577.

17. **Copper, GM**. 2000. The Cell: A Molecular Approach, 2nd ed, Sinauer Associates, Sunderland, MA.

18. **Daegelen, P., Studier, FW., Lenski, RE., Cure, S., Kim, JF.** 2009. Tracing ancestors and relatives of Escherichia coli B, and the derivation of B strains REL606 and BL21(DE3). J Mol Biol. **394**(4):634-43.

19. **Dukhande, V.V., Kawikova, I., Bothwell, A.L.M., Lai, J.C.K.** 2013. Neuroprotection against neuroblastoma cell death induced by depletion of mitochondrial glutathione. Apoptosis. **18**(6):702-712.

20. **Eisel, U. Jarausch, W., Goretski, K., Henschen, A., Engels, J., Weller, U., Hudel, H., Habermann, E., Niemann, H.** 1986. Tetanus toxin: primary structure, expression in E. coli, and homology with botulinum toxins. The EMBO Journal. 5(**10**):2495-2502.

21. **Engleberg, N.C. et. al.** 2013. Schaechter's Mechanisms of microbial Disease 5th Ed., Lippincott, Baltimore, MD.

22. **Falnes, P.O., Sandvig, K.** 2000. Penetration of protein toxins into cells. Current Opinion in Cell Biology. **12**:407-413.

23. **Fraser, J.D.** 2011. Clarifying the mechanism of superantigen toxicity. PLoS Biol. doi:10.1372/journal.pbio.1001145.

24. GE Healthcare. 2010a. Gel filtration. GE Healthcare, Pittsburgh, PA.

25. GE Healthcare. 2010b. Size Exclusion Chromatography. GE Healthcare, Pittsburgh, PA.

26. **Goebel, W., Chakraborty, T., Kreft, J.** 1988. Bacterial hemolysins as virulence factors. Antonie van Leeuwenhoek. **54**:453-463.

27. **Gorbach, S.L.** 2012. Clinical Infectious Diseases. Oxford Journals **55** (9).

28. **Graham, J.M.** 2002. Preparation of crude subcellular fractions by differential centrifugation. The Scientific World. **2**:1638-1642.

29. **Harrington, D.J.** 1996. Bacterial collagenase and collagen-degrading enzymes and their potential role in human disease. Infect. Immun. **64**:1885.

30. **Hayashi, T., McMahon, H., Yamasaki, S., Binz, T., Hata, S., Hata, Y., Sudhof, T.C., Niemann, H.** 1994. Synaptic vesicle membrane fusion complex: action of clostridial neurotoxins on assembly. EMBO. **13**:5051-5061.

31. **Herreros, J., NG, T., Schiavo, G.** 2001. Lipid rafts act as specialized domains for tetanus toxin binding and internalization into neurons. Molecular Biology of the cell. **12**:2947-2960.

32. **Humeau, Y. Doussau, F. Grant, N.J., Poulain, B.** 2000. How botulinum and tetanus neurotoxins block neurotransmitter release. Biochimie. **82**:427-446.

33. IBA. 2012. Expression and purification of proteins using double tag (*Strep*-tag/6x*Histidine*-tag). Goettingen, Germany.

34. **Ivarsson, M., E., Leroux, J., C., Castagner, B.** 2012. Targeting bacterial toxins. Angew Chem Int Ed. **51**:4024-4045.

35. **Kirchhausen, T.** 2000. Three ways to make a vesicle. Nature. **1**:187-198

36. **Lalli, Giovanna. Bohnert, S. Deinhardt, K., Verastegui, C., Schiavo, G.** 2003. The journey of tetanus and botulinum neurotoxins in neurons. TRENDS in Micro. **11**:431-437.

37. **Lee, J.S., Zhang, M.H., Yun, E.K., Geum, D., Kim, K., Kim, T.H., Lim, Y.S., Seo, J.S**. 2005. Heat shock protein 27 interacts with vimentin and prevents insolubilization of vimentin subunits induced by cadium. Experimental and Molecular Medicine. **37**(5): 427-435.

38. **Lemichez,E., Barbieri, J.T.** 2013. General aspects and recent advances on bacterial protein toxins. Cold Spring Harb Perspect doi:10.1101/cshperspect.a013573.

39. **Li, L., Chin, L.-S.** 2003. The molecular machinery of synaptic vesicle exocytosis. Cell Mol Life Sci. **60**:942-960.

40. **Li, Y.F.,Wang, D.D., Zhao, B.W., Wang, W., Huang, CY., Chen, Y.M., Zheng, Y., Keshari R.P., Xia, J.C., Zhou, Z.W.** 2012. High level of COP1 expression is associated with poor prognosis in primary gastric cancer. Int J Biol Sci. **8**(8):1168-1177.

41. **Los, F.C.O., Randis, T.M., Aroian, R.V., Ratner, A.J.** 2013. Role of pore-forming toxins in bacterial infectious diseases. Microbiol Mol Biol. **77**:173–207.

42. **Martinez-Arca, S. Alberts, P. Zahraoui, A. Louvard, D. Galli, T.** 2000. Role of Tetanus neurotoxin insensitive vesicle-associated membrane protein (TI-VAMP) in vesicular transport mediating neurite outgrowth. JCB. **149**(4):889-899.

43. **Murphy, J.R.** 2011. Mechanism of Diphtheria toxin catalytic domain delivery to the eukaryotic cell cytosol and the cellular factors that directly participate in the process. Toxins. **3**:294-308.doi:10.3390/toxins3030294.

44. **Murray, P.R., Rosenthal, K.S., Kobayashi, G.S., Pfaller, M.A**. 2002. *In* Grigg, L.L. (ed) Medical Microbiology, 4th ed, Mosby, St. Louis, MI.

45. **Montecucco, C., Schiavo, G.** 1994. Mechanism of action of tetanus and botulinum neurotoxins. Molecular Microbiology. **13**:1-8.

46. **Montesano R, Pepper MS, Mohle-SteinleinU, Risau W, Wagner EF, Orci L.** 1990. Increased proteolytic activity is responsible for the aberrant morphogenetic behavior of endothelial cells expressing the middle T onco-gene. Cell **62:** 435–445.

47. **Novick, P., Field, C., Schekman, R.** 1980. Identification of 23 complementation groups required fro post-translational events in the secretory pathway. Cell. **21**:205-25.

48. **Odumosu, O., Nicolas, D., Yano, H., Langridge, W.** 2010. AB Toxins: A paradigm switch from deadly to desirable. Toxins. **2**(7):1612-1645

49. **Pellet, S.** 2013. Progress in the cell based assays for Botulinum neurotoxin detection. Curr Top Microbiol Immunol. **364**:257-285.

50. **Pellizzari, R. Mason, S. Shone, C.C. Montecucco, C**. 1997. The interaction of synaptic vesicle-associated membrane protein/synaptobrevin with botulinum neurotoxins D and F. FEBS. **409**:339-342.

51. **Popoff, V., Adolf, F., Brugger, B., Wieland, F.** 2011. COP1 budding within the Golgi stack. Cold Spring Harb Perspect. doi:10.1101/cshperspect.a005231

52. **Proft, T., Fraser, J.D.** 2003. Bacterial superantigens. Clin Exp Immunol. **133**:299-306.

53. **Proux-Gillardeaux, V., Rudge, R., Galli, T.** 2005. The tetanus neurotoxin-sensitive and insensitive routes to and from the plasma membrane: fast and slow pathways? Traffic. **6**:366-373.

54. **Ratts, R. Trujillo, C., Bharti, A., Vanderspek, J.C., Harrison, R., Murhpy, J.R.** 2005. A conserved motif in transmembrane helix 1 of diptheria toxin mediates catalytic domain delivery to the cytosol. Proc Natl Acad Sci USA. **102**: 15635-15640.

55. **Ratts, R., Zeng, H., Berg, E.A., Blue, C., McComb, M.E., Costello, C.E., Vanderspeck, J.C., Murphy, J.R.** 2003. The cytosolic entry of diphtheria toxin domain requires a host cell cytosolic translocation factor complex. J Cell Bio. **160**:1139-1150.

56. **Rhee, P., Nunley, M.K., Demetriades, D., Velmahos, G., Doucet, J.J.** 2005. Tetanus and trauma: A review and recommendations. J Trauma. **58**:1082-1088.

57. **Rizzoli, S.O.** Synaptic vesicle recycling: steps and principles. EMBO.DOI 10.1002/embj.201386357

58. **Sakurai,J., Nagahama, M., Oda, M.** 2004. Clostridium perfringens alpha-toxin: characterization and mode of action. J Biochem. **136**:569-574.

59. **Salinas, S., Shiavo, G., Kremer, EJ.** 2010. A hitchhiker's guide to the nervous system: the complex journey of viruses and toxins. Nat. Rev. Microbiol. **8**:645-655.

60. **Schiavo, G., Matteoli, M., Montecucco, C.** 2000. Neurotoxins affecting neuroexocytosis. American Physiological Society. **80**:717-750.

61. **Sheff, D., Lowe, M., Kreis, T.E., Mellman,I.** 1996. Biochemical heterogeneity and phosphorylation of coatomer subunits. J. Biol. Chem. **271**:7230-7236.

62. **Slater, L.H., Hett, E.C., Clatworthy, A.E., Mark, K.G., Hung, D.T.** 2013. CCT chaperonin complex is required for efficient delivery of anthrax toxin into the cytosol of host cells. PNAS. **110**:9932-9937.

63. **Sudhof, T.C., Rizo, J.** 2011. Synpatic Vesicle Exocytosis. Cold Spring Harb Perspect. doi:1101/cshperspect.a005637.

64. **Sun, J., Collier, R.J.** 2010. Disulfide bonds in the ectodomain of anthrax toxin receptor 2 are required for the receptor-bound protective-antigen pore to function. PLoS One. **5.**

65. **Szul, T., Sztul, E.** 2011. COP1I and COP1 traffic at the ER-Golgi interface. Physiology. **28**:348-364.

66. **Tamayo, A.G., Bharti, A., Trukillo, C., Harrison, R., Murphy, J.R.** 2008. COP1 coatomer complex proteins facilitate the translocation of anthrax lethal factor across vesicular membranes in vitro. Proc Natl Acad Sci. **105**:524-529.

67. **Tamayo, A.G., Slater, L. Taylor-Parker, J., Bharti, A., Harrison, R., Hung, D.T., Murphy, J.R.** 2011. GRP78(BiP) facilitates the cytosolic delivery of anthrax lethal factor (LF) *in vivo* and functions as an unfoldase *in vitro*. Molecular Microbiology. **81**(5):1390-1401.

68. **Teter, K.** 2013. Toxin instability and its role in toxin translocation from the endoplasmic reticulum to the cytosol. Biomolecules. **3**:997-1029.

69. **Teujillo,C., Taylor-Parker, J., Harrison, R., Murphy, J.R.** 2010. Essential lysine residues within transmembrane helix 1 of diphtheria toxin facilitate COP1 binding and catalyst domain entry. Mol Microbiol. **76**(4): 1010-9.

70. ThermoScientific. 2009. Thermo Scientific Pierce Cell Lysis Technical Handbook.

71. **Turton, K., Chaddock, J.A., Acharya, K.R.** 2002. Botulinum and tetanus neurotoxins: structure, function and therapeutic utility. TiBS. **27**(11), 552-558.

72. **Wernick, N., L., B., Chinnapen, D., J., F., Cho, J.A., Lencer, W., I.** 2010. Cholera toxin: an intracellular journey into the cytosol by way of the endoplasmic reticulum. Toxins. **2**:310-325.doi: 10.3390/toxins2030310.

73. World Health Organization. 2014. Vaccine-preventable diseases: monitoring system 2014 global summary. Tech. Rep.

74. **Wright, J.F., Pernollet, M., Reboul, A., Aude, C., Colomb, M.G.** 1992. Identification and partial characterization of a low affinity metal-binding site in the light chain of tetanus toxin. JBC. **27**(13): 9053-9058.

75. **Yowler, B.C., Kensinger, R.D.** 2002. Botulinium neurotoxin A activity is dependent upon the presence of specific gangliosides in neuroblastoma cells expressing synaptotagmin. I. JBC. **277**:32815-32819.

Appendix A

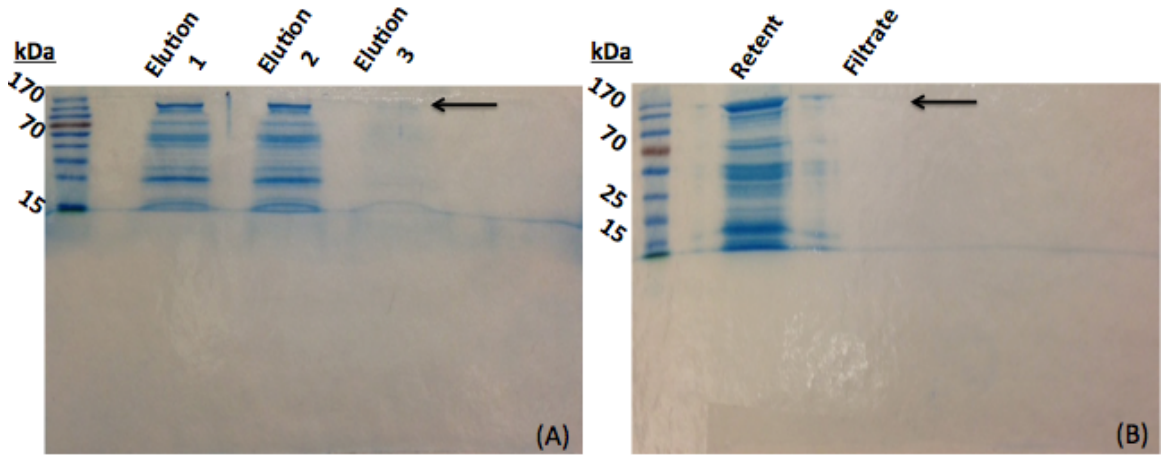

Appendix A. Panel 1. **Purification Scheme A. Nickel Affinity Chromatography, SEC, and Protein Concentration.** 1.5 L of BL21 pET28TeNT$_{RY}$ was induced to yield soluble lysate that was purified by HisPur-Ni-NTA resin (**A)**. Elutions 1 and 2 containing TeNT$_{RY}$ were combined and concentrated (**B**).

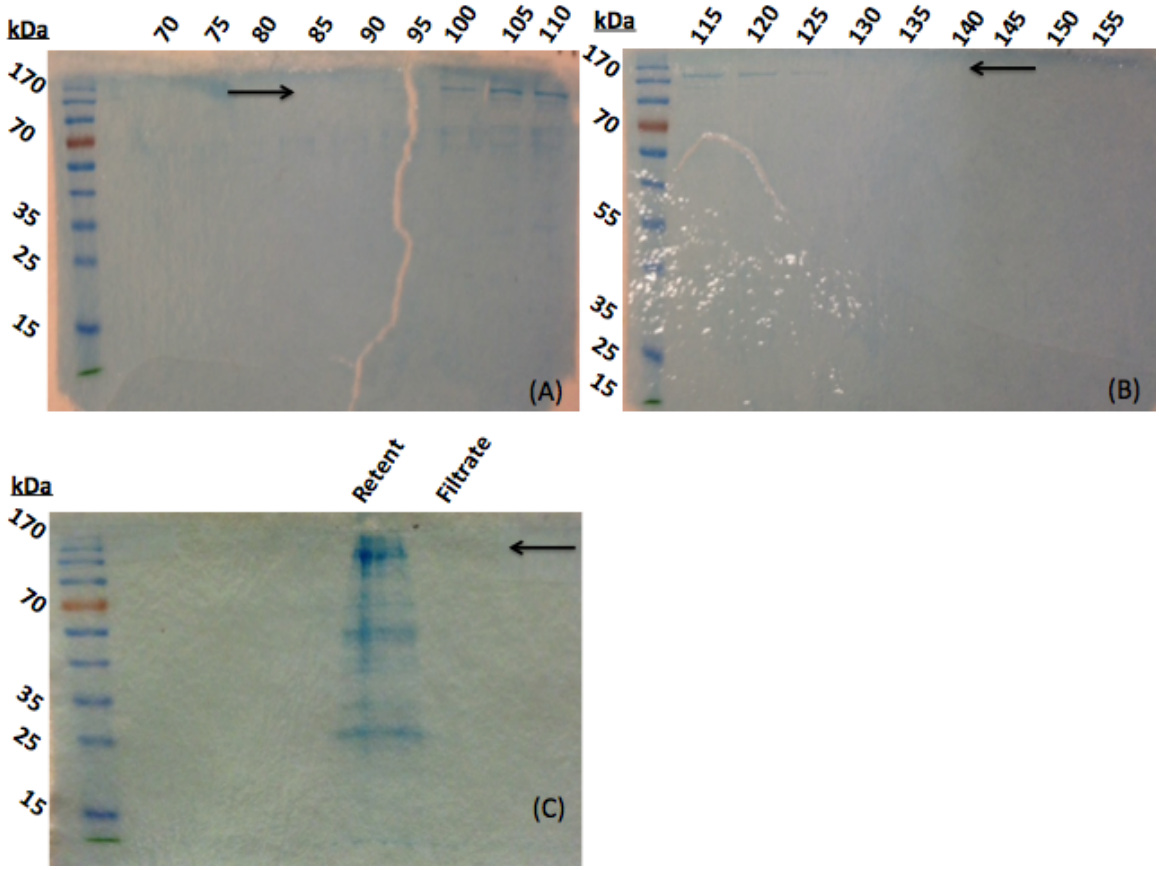

Appendix A. Panel 2. Purification Scheme A. SEC, Protein Concentration. The 600 µl concentrated protein (**Appendix A, Panel 1**) was subjected to an additional SEC purification. To increase the yield of $TeNT_{RY}$, the fractions were collected every 2.5 ml. Very faint 150-kDa $TeNT_{RY}$ bands are present in fractions ranging from 95 ml to 125 ml (**A, B**). When the fractions were combined and concentrated (**C**), an insubstantial amount of $TeNT_{RY}$ had been recovered.

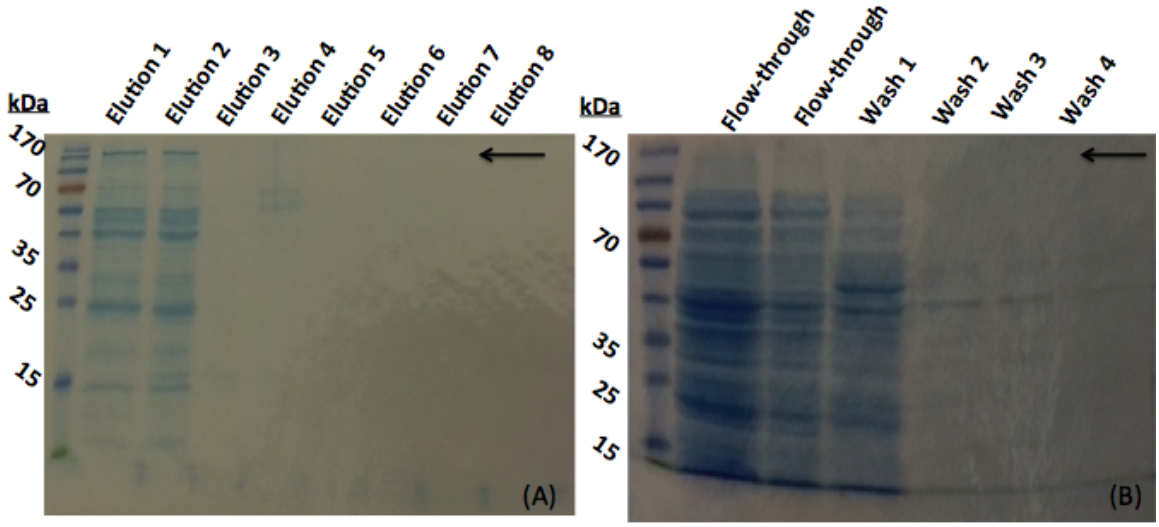

Appendix A. Panel 3. Purification Scheme A. Nickel Affinity Chromatography. Soluble lysate produced from 1 L of BL21pET28TeNT$_{RY}$ was applied to HisPur-Ni-NTA resin. The column was washed four times with 20 ml of wash buffer (**B**) and eight 3 ml elutions were performed (**A**). A minimal amount of TeNT$_{RY}$ was present in elutions 1 and 2. Analysis of HisPur-Ni-NTA resin did not show any TeNT$_{RY}$ present in the washes or flow-through, indicating the resin is functioning properly.

Appendix B

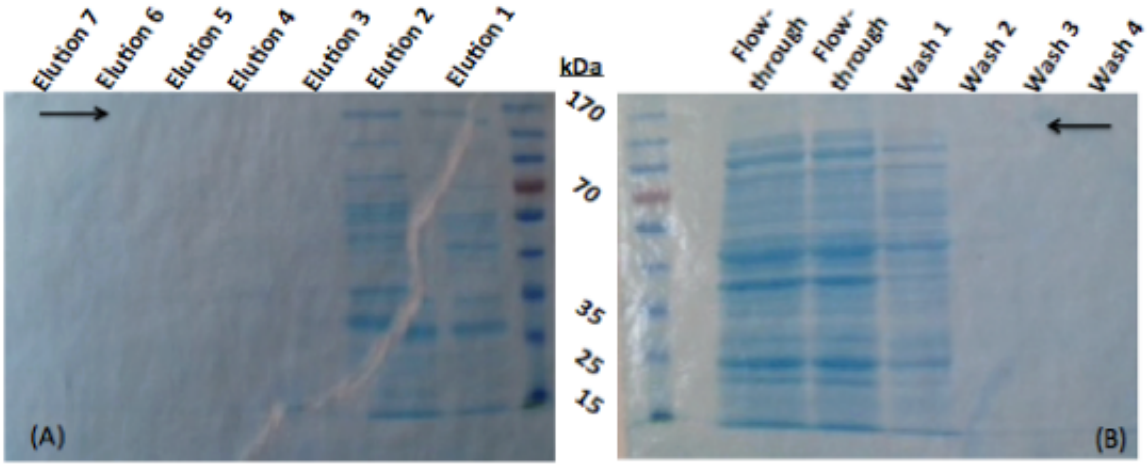

Appendix B. Panel 1. Purification Scheme B. Nickel Affinity Chromatography, Dialysis. Cellular pellets obtained from expressing 1.2 L of BL21pET28TeNTRY, frozen at -80°C to increase cell lysis. The cl lysate was applied to HisPur-Ni-NTA resin and subjected to four 20 ml washes and seven 3 ml elutions. A very small amount of $TeNT_{RY}$ is present in Elutions 1 and 2 (**A**) while $TeNT_{RY}$ is absent in the resin analysis (**B**).

Appendix C

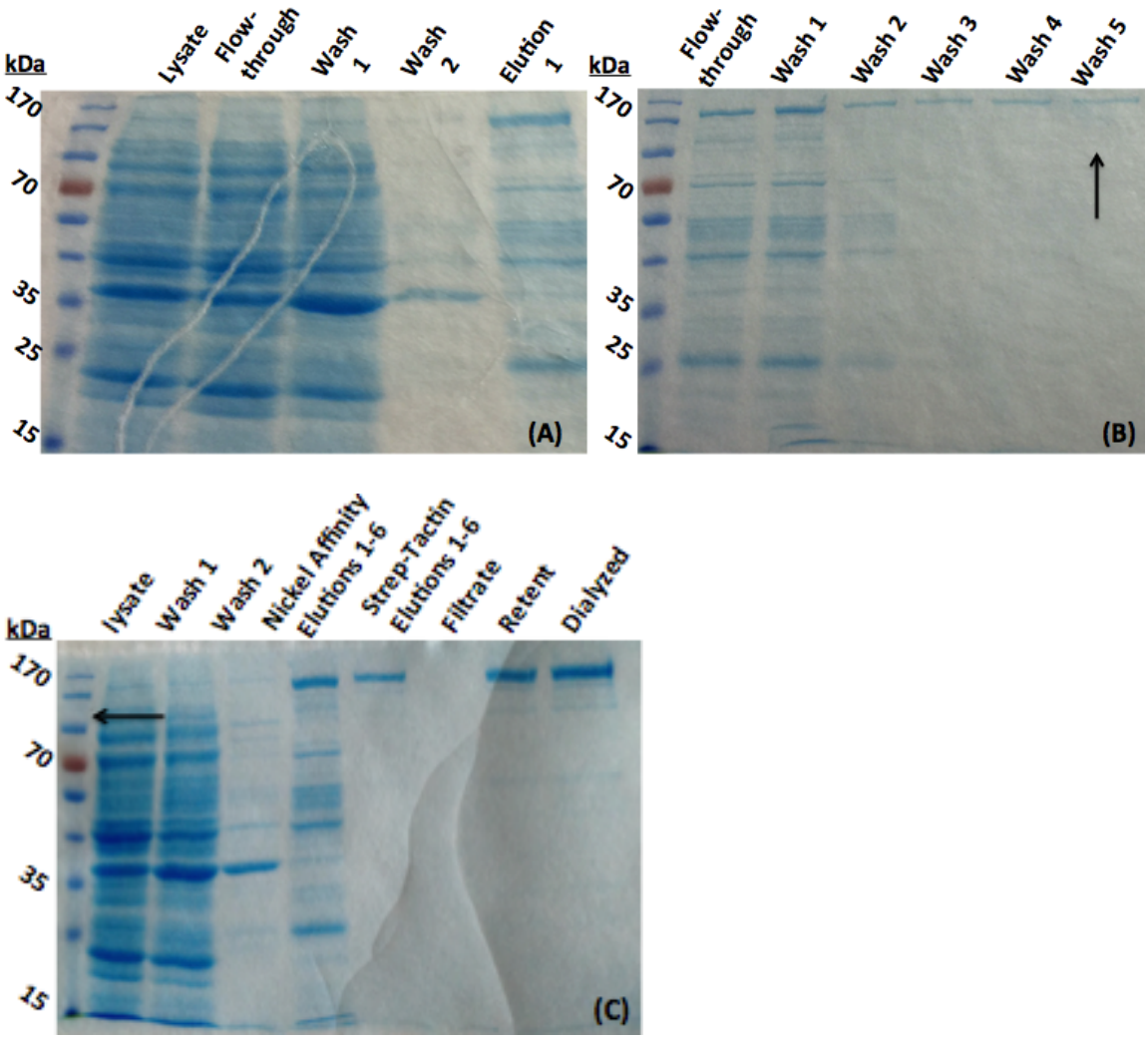

Appendix C. Panel 1. Purification Scheme C. Nickel Affinity Chromatography, Strep-tactin Chromatography, Protein Concentration and Dialysis. Cellular pellets obtained from 1.6 L of BL21 pET28TeNT$_{RY}$ were purified by (**A**) nickel affinity chromatography. The Ni-NTA resin was washed twice (20 ml then 5 ml) and the resulting 10 ml elution was further purified by Strep-tactin chromatography. The elutions containing TeNT$_{RY}$ were combined, concentered (**B**) and dialyzed (**C**).

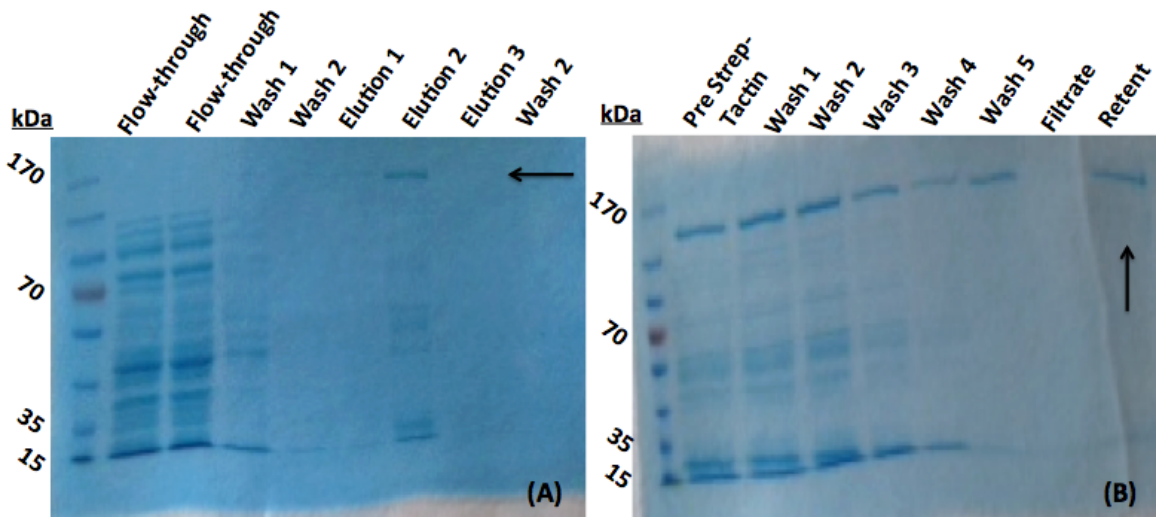

Appendix C. Panel 2. Purification Scheme C. The expression of 1 L of BL21 pET28TeNT$_{RY}$ and freezing of cellular pellets was repeated as previously described. The lysate was initially purified by nickel affinity chromatography (**Appendix C, Panel 2**) followed by purification by Strep-Tactin chromatography (**Appendix C, Panel 2**). The resulting Strep-tactin elutions were pooled, concentrated and dialyzed (**Appendix C, Panel 2**). According to the results of the BCA Assay, the final, dialyzed sample contained 53 nM of relatively pure TeNT$_{RY}$. While this is a sufficient amount to proceed to SK-N-SH binding assays, the purification protocol needs to be further optimized to produce a more pure, concentrated TeNT$_{RY}$ product.

Appendix D

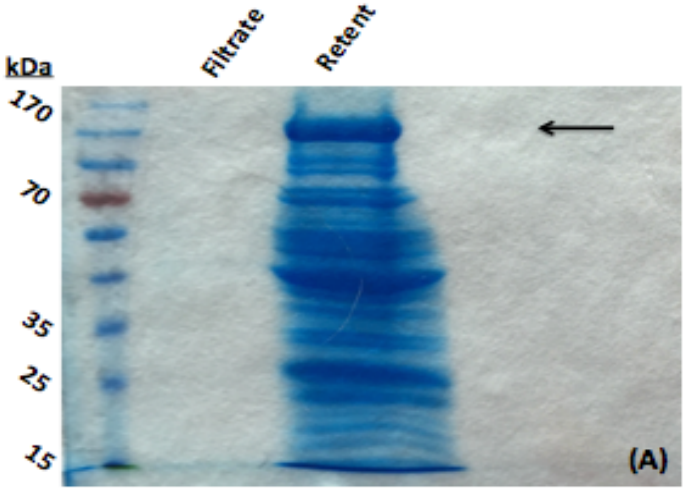

Appendix D. Panel 1. Purification Scheme D. Lysate obtained from 1.8 liters of BL21 pET28TeNT$_{RY}$ was purified by sequential affinity chromatography methods (Nickel Affinity and Strep-tactin). The final elutions were pooled and concentrated. While there is a significant amount of TeNT$_{RY}$ in the retent, a significant amount of impurities are also present.

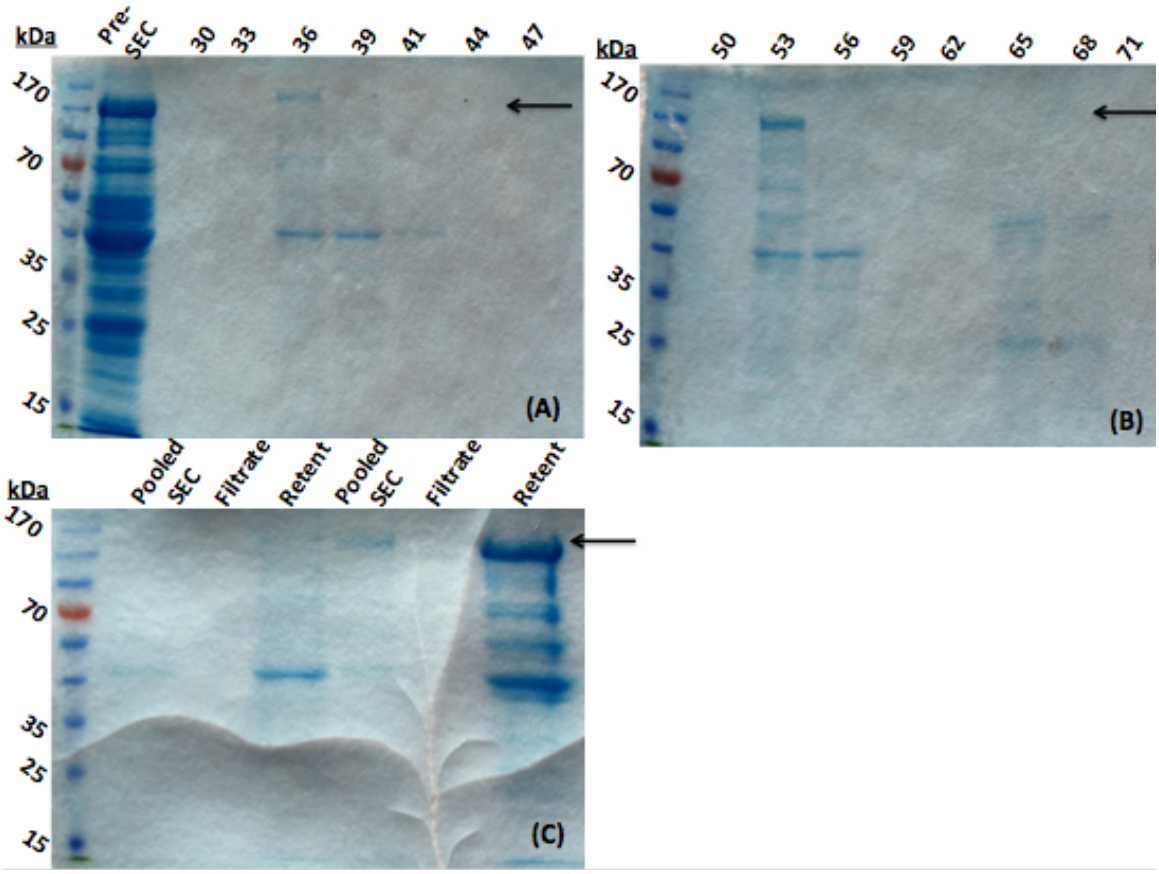

Appendix D. Panel 2. Size exclusion chromatography was performed on the concentrated protein sample (**Appendix D, Panel 1**) to reduce the amount of impurities present. The fractions containing the 150-kDa protein (**A,B**) were combined and concentrated (**C**). A large amount of $TeNT_{RY}$ and impurities were present.

Appendix E

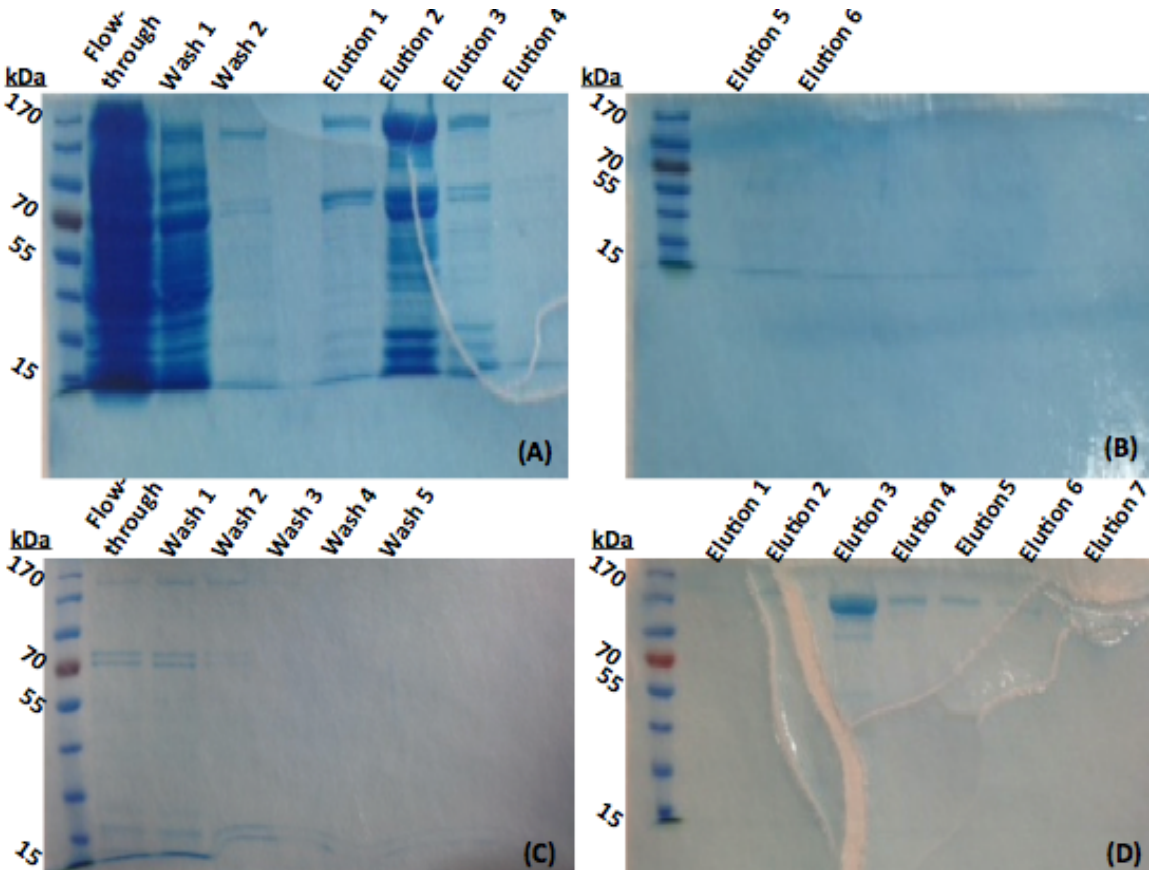

Appendix E. Panel 1. Optimized $TeNT_{RY}$ Purification. Soluble BL21 pET28$TeNT_{RY}$ lysate generated from the French Press was initially purified by Nickel Affinity Chromatography. Following two 25 ml washes and six 2.5 ml elutions (**A,B**), Elutions 1-4 were combined and further purified by Strep-tactin chromatography. Five 1 ml washes followed by 6 0.5 elutions were performed (**C,D**). $TeNT_{RY}$ is present in Elutions 2-6.

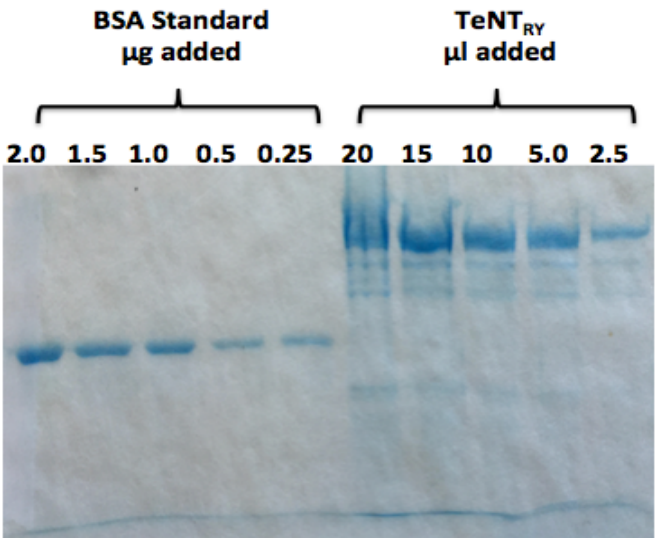

Appendix E. Panel 2. Optimized TeNT$_{RY}$ Purification. Densitometry. SDS-PAGE depicting band density of known concentrations of the BSA standard (2.0 µg-0.25 µg) was compared to unknown concentrations of purified TeNT$_{RY}$.